Deciphering the significant role of biological ice nucleators in precipitation at the organic molecular level

Mutong Niu[1], Wei Hu[1], Shu Huang[2], Jie Chen[3], Shujun Zhong[1], Ziye Huang[1], Peimin Duan[1], Xiangyu Pei[4], Jing Duan[5], Kai Bi[6], Shuang Chen[2], Rui Jin[7], Ming Sheng[1], Ning Yang[1], Libin Wu[1], Junjun Deng[8], Jialei Zhu[9], Fangxia Shen[10], Zhijun Wu[11], Daizhou Zhang[12], and Pingqing Fu[2]

[1]Tianjin University
[2]Institute of Surface-Earth System Science, Tianjin University
[3]ETH Zürich
[4]Zhejiang University
[5]CMA Cloud-Precipitation Physics and Weather Modification Key Laboratory, CMA Weather Modification Centre
[6]Beijing Weather Modification Center
[7]School of Earth System Science, Tianjin University
[8]Institute of Surface-Earth System Science, School of Earth System Science, Tianjin University
[9]Tianjin Univeristy
[10]Beihang University
[11]Peking University
[12]Prefectural University of Kumamoto

April 12, 2024

Abstract

Biological particles, as a fraction of organic particles, potentially play a crucial role in ice nucleation processes. However, the contributions and relationships of biological components and organic matter (OM) to atmospheric ice nucleation are still largely unexplored. Here, droplet freezing assays, high-throughput sequencing technology and ultrahigh-resolution mass spectrometry were performed to detect the INPs, microorganisms and OM molecules in precipitation collected at the summit of Mt. Lu, China, respectively. Results revealed a predominant biological composition (71.7% and 93.2%) of total and nanoscale INPs ($<$ 0.22 μm) at temperatures above -15°C. Specifically, bacterial INPs accounted for 36.1% of the biological INPs at temperatures above -15degC. A notable correlation between sulfur-containing compounds, mainly proteinaceous and lignin-like substances, and INPs was uncovered, with a co-occurrence network linking these compounds to Gram-positive bacteria and Agaricomycetes. This study underscored the possible significance of sulfur-containing compounds in biological INP efficiency, which could further help shed light on the ice nucleation mechanisms and potential sources of biological INPs.

Hosted file

`Revised Main Manuscript-Clean Version.docx` available at https://authorea.com/users/765538/articles/788407-deciphering-the-significant-role-of-biological-ice-nucleators-in-precipitation-at-the-organic-molecular-level

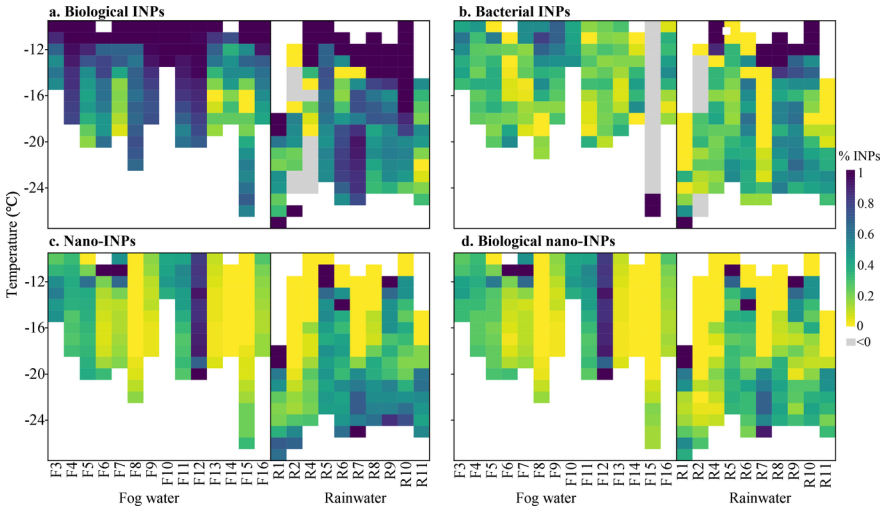

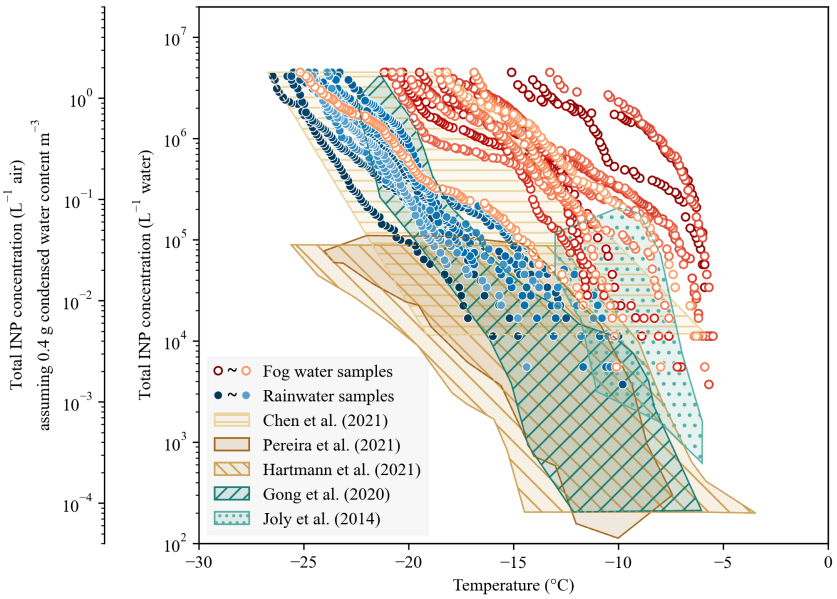

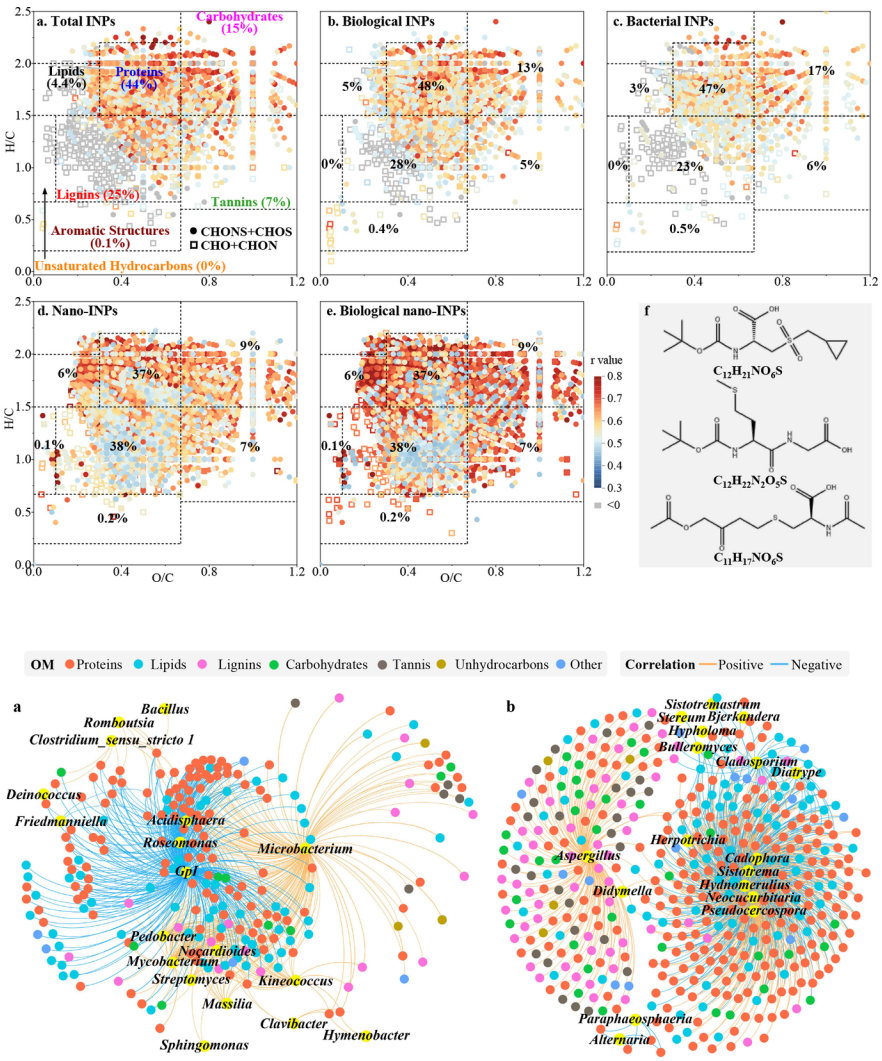

Deciphering the significant role of biological ice nucleators in precipitation at the organic molecular level

Mutong Niu[1], Wei Hu[1, *], Shu Huang[1], Jie Chen[2], Shujun Zhong[1], Ziye Huang[1], Peimin Duan[1], Xiangyu Pei[3], Jing Duan[4], Kai Bi[5], Shuang Chen[1], Rui Jin[1], Ming Sheng[1], Ning Yang[1], Libin Wu[1], Junjun Deng[1], Jialei Zhu[1], Fangxia Shen[6], Zhijun Wu[7], Daizhou Zhang[8], Pingqing Fu[1, *]

[1]Institute of Surface-Earth System Science, School of Earth System Science, Tianjin University, Tianjin 300072, China, [2]Institute for Atmospheric and Climate Science, ETH Zürich, Zurich 8092, Switzerland, [3]College of Environmental and Resource Sciences, Zhejiang Provincial Key Laboratory of Organic Pollution Process and Control, Zhejiang University, Hangzhou 310058, China, [4]State Key Laboratory of Severe Weather & Key Laboratory for Cloud Physics, Chinese Academy of Meteorological Sciences, Beijing 100081, China, [5]Beijing Key Laboratory of Cloud, Precipitation, and Atmospheric Water Resources, Beijing Weather Modification Office (BWMO), Beijing 100089, China, [6]School of Energy and Power Engineering, Beihang University, Beijing 102206, China, [7]State Key Joint Laboratory of Environmental Simulation and Pollution Control, College of Environmental Sciences and Engineering, Peking University, Beijing 100081, China, [8]Faculty of Environmental and Symbiotic Sciences, Prefectural University of Kumamoto, Kumamoto 862-8502, Japan

Corresponding author: W. Hu (huwei@tju.edu.cn), P. Fu (fupingqing@tju.edu.cn)

Key Points:

- Biological materials predominated in ice nucleating particles (INPs) identified in precipitation.
- Sulfur-containing compounds, associated with specific microbial taxa, likely acted as efficient INPs in precipitation.
- This study preliminarily established an understanding of the connections between INPs, organic matter, and microorganisms.

Abstract

Biological particles, as a fraction of organic particles, potentially play a crucial role in ice nucleation processes. However, the contributions and relationships of biological components and organic matter (OM) to atmospheric ice nucleation are still largely unexplored. Here, droplet freezing assays, high-throughput sequencing technology and ultrahigh-resolution mass spectrometry were performed to detect the INPs, microorganisms and OM molecules in precipitation collected at the summit of Mt. Lu, China, respectively. Results revealed a predominant biological composition (71.7% and 93.2%) of total and nanoscale INPs (< 0.22 μm) at temperatures above −15°C. Specifically, bacterial INPs accounted for 36.1% of the biological INPs at temperatures above −15°C. A notable correlation between sulfur-containing compounds, mainly proteinaceous and lignin-like substances, and INPs was uncovered, with a co-occurrence network linking these compounds to Gram-positive bacteria and Agaricomycetes. This study underscored the possible significance of sulfur-containing compounds in biological INP efficiency, which could further help shed light on the ice nucleation mechanisms and potential sources of biological INPs.

Plain Language Summary

Ice nucleating particles (INPs) are particles that facilitate the freezing of water at temperatures above the homogenous freezing point, impacting cloud formation and precipitation processes in the atmosphere. This study identified different types of INPs, microbes and organic matter in precipitation sampled from Mt. Lu in southeastern China and investigated the connections between them. The findings suggested that a significant portion of INPs were of biological origin. Sulfur-containing compounds likely played an important role in ice nucleation, which may originate from certain microbial taxa. This study will help us understand the role of microbes and organic molecules in ice formation, which has broader implications in areas like preserving biological materials at low temperatures or even facilitating artificial snow production.

1. Introduction

Ice nucleation and subsequent ice crystal formation in clouds can affect the global hydrological cycle by altering cloud and precipitation formation, as well as affect the Earth's solar radiation balance (DeMott et al., 2010; Lohmann & Feichter, 2005). As a result, ice nucleating particles (INPs) which aid the heterogeneous ice nucleation have received a great deal of attention (Kanji et al., 2017; Vali et al., 2015). To date, biological materials, mineral dust, crystalline salts, volcanic ash and carbonaceous combustion products (e.g., soot particles) have been identified as INPs (Hoose & Möhler, 2012; Kilchhofer et al., 2021; Möhler et al., 2008; Wise et al., 2012). Among them, biological materials (e.g., bacteria, fungal spores) or biological macromolecules (e.g., proteinaceous substances, saccharides, and lipids) exhibit the highest ice nucleation activity (INA) (Conen et al., 2011; Pummer et al., 2015). Some bacterial INPs, notably *Pseudomonas syringae* (Arny et al., 1976), *Ps. fluorescens* (Obata et al., 1987), *Ps. viridiflava* (Obata et al., 1989), *Erwinia ananas* (Hew & Yang, 1992), *Er. uredovora* (Obata et al., 1989) and *Xanthomonas campestris* (Kim et al., 1987), were particularly effective at promoting ice

nucleation at above −10°C. Certain strains of *Ps. syringae*, known as highly active ice nucleators, even can initiate freezing at temperatures as high as −1.8°C (Maki et al., 1974). Fungi such as certain strains of *Fusarium* sp. (Kunert et al., 2019), *Mortierella alpine* (Iannone et al., 2011), and *Cladosporium* spores (Fröhlich-Nowoisky et al., 2015) have also demonstrated INA. The ice nucleation mechanisms in these microbial INPs are associated with proteins and polysaccharides (Morris et al., 2013). Additional biological materials, including pollen, lichens, and algae, are capable of initiating freezing at elevated temperatures (Christner, 2010; Duan et al., 2023; Karimi et al., 2019). Due to the remarkable INA of biological INPs (bio-INPs), the concentrations, compositions and influencing factors of bio-INPs in various environments have been widely documented (Che et al., 2019; Chen, Wu, Wu, et al., 2021; Huang et al., 2021; Pereira et al., 2021).

Bio-INPs, as a part of organic INPs, have received limited attention regarding their INA from the perspective of organic matter (OM), especially at the molecular level. Past studies have primarily assessed the activities of bulk OM in environmental samples, e.g., marine aerosols (Wilson et al., 2015) and agricultural soil dust (Conen et al., 2011; Hill et al., 2016; O'Sullivan et al., 2014; Tobo et al., 2014), utilizing heating treatment or hydrogen peroxide digestion combined with droplet freezing measurements. Diverse OM components, such as cellulose (Hiranuma et al., 2019), lipids (Steinke et al., 2020), lignin (Bogler & Borduas-Dedekind, 2020), humic or fulvic acids (Klumpp et al., 2022; Wang & Knopf, 2011), humic-like substances (HULIS) (Chen, Wu, Zhao, et al., 2021) and proteinaceous materials (Christner, 2010; Watabe et al., 1993), were found to possess significant INA. The INA of these OM components exhibits considerable variation. For instance, the average freezing temperatures of fulvic acid and lignins ranged from −13°C to −8°C (Borduas-Dedekind et al., 2019), while the ice nucleation temperature of cellulose or polysaccharides (i.e., starches) was lower than −20°C (Hiranuma et al., 2019; Hiranuma et al., 2015; Steinke et al., 2020). Some proteinaceous materials derived from microorganisms exhibited notably efficient INA (Cascajo-Castresana et al., 2020; Maki et al., 1974; Schnell & Vali, 1976). Specifically, iron storage proteins and ice nucleating proteins initiated ice formation at −4°C and −1.8°C, respectively (Cascajo-Castresana et al., 2020; Maki et al., 1974; Schnell & Vali, 1976). Nevertheless, the precise molecular-level compositions of bio-INPs remain comparatively less studied, requiring further investigation to elucidate the underlying ice nucleation mechanisms.

Ice crystal formation in clouds plays a crucial role in Earth's radiative balance and hydrological cycle, prompting extensive global research on INPs in clouds and precipitation (Failor et al., 2022; Petters & Wright, 2015). Previous studies have utilized the abundances of INPs in various precipitation samples, such as rain, snow, fog, and hail, to estimate INPs in clouds (Beall et al., 2020; Martin et al., 2019; Michaud et al., 2014). While precipitation samples may collect additional INPs in the below-cloud atmosphere and undergo heterogeneous chemistry through gas adsorption or absorption (Lim et al., 2010), they largely resemble cloud water, particularly in clean areas (Hu et al., 2017). INPs in precipitation from clean and high-altitude regions face fewer environmental interferences, offering a more direct reflection of cloud ice nucleation processes. Additionally, collecting precipitation samples is more convenient than cloud water collection for characterizing atmospheric water properties.

As a result, numerous studies have focused on INP concentrations in precipitation at mountainous sites (Ahern et al., 2007; Stopelli et al., 2017). Conen et al. (2015) revealed

seasonal variations in INP concentrations at −8°C at Jungfraujoch, with higher levels in summer. The INPs increases coincided with high wind speeds and air masses with little or no precipitation (Stopelli et al., 2016). Wind direction and air mass trajectories significantly affected INP concentrations and biogenic contributions at Jungfraujoch (Creamean et al., 2019) and southeastern Louisiana (Joyce et al., 2019). In some instances, anthropogenic factors, like PM_{10} and rain acidification, have influenced INP concentrations (Lacher et al., 2018; Pouzet et al., 2017). The Sierra Nevada Mountains in California, renowned for their orographic cloud formation, have undergone thorough studies regarding INP characteristics (Creamean et al., 2014; Creamean et al., 2016). Long-distance transported dust and biological particles were key components of INPs, significantly influencing orographic precipitation in the western United States (Creamean et al., 2013). At Puy de Dôme, biological materials also constituted major components of INPs, representing over 60% at −10°C (Joly et al., 2014; Testa et al., 2021). Nevertheless, microorganisms with known ice nucleation ability represented only a minority of bio-INPs in precipitation (Zhang et al., 2020), and many unknown bio-INPs remain to be explored. Additionally, nanoscale biological fragments have been found to possess ice nucleation capabilities in precipitation samples (O′Sullivan et al., 2015; Wilson et al., 2015). It is important to note that organisms, as a fraction of organic matter, continuously release various organic substances during their metabolic processes. It has been suggested that organic matter associated with biological substances may have high ice nucleating abilities in soils (Tobo et al., 2019). However, the specific connection between organic molecules and bio-INPs at the molecular level in precipitation remains unexplored.

Mt. Lu, situated in the middle and lower reaches of Yangtze River in China, features high altitudes and deep valleys, resulting in significant vertical and horizontal climatic variations. Due to its unique geography, Mt. Lu frequently experiences meteorological phenomena such as rime, snow rime, and rain rime (Guo et al., 2019). Therefore, Mt. Lu has been the site of comprehensive observational studies focusing on the physical properties of precipitation and aerosols (Huang et al., 2018; Li et al., 2015; Sun et al., 2016). Here, to assess the abundances of INPs in clouds and the contribution of biological and organic fractions to INPs as well as their associations, precipitation (including rain and fog water) samples were collected from a relatively clean and high-altitude mountain site, Mt. Lu, in southeastern China. The abundances and compositions of INPs including bio-INPs, bacterial INPs, nanoscale INPs (nano-INPs) and biological nano-INPs were determined by droplet freezing assays coupled with corresponding pretreatments. Microbial and organic compositions were measured with high-throughput sequencing technology and ultrahigh-resolution Fourier transform ion cyclotron resonance mass spectrometry (FT-ICR MS), respectively. This study aims to provide more information on the components, sources and potential atmospheric processes of INPs, and especially to clarify the relationships among INPs, microorganisms and organic molecules.

2. Materials and Methods

2.1. Observation site and sample collection

Precipitation including rainwater and fog water samples were collected at the summit of Mt. Lu (29.58°N, 115.98°E, 1165 m a.s.l.) from November to December 2019. Mt. Lu is located in the southeast of China and it has frequent cloudy weather and rainfall events throughout the year due to the influence of the subtropical monsoon. Fog water samples were collected into Teflon

bottles using a Caltech Active Cloudwater Collector (CASCC2) following the operation protocol. Rainwater samples were deposited directly into Teflon beakers. After collection, the samples were transferred to brown polyethylene bottles and stored at −20°C. Meteorological data were recorded by an automatic meteorological monitoring station (Gill MetPak, UK), and hourly air quality data including air quality index (AQI), $PM_{2.5}$, PM_{10}, NO_2, O_3, SO_2 and CO were obtained from the nearest air quality monitoring station (29.57°N, 115.98°E), which is 20 m away from the sampling site. All air quality data were downloaded from China National Environmental Monitoring Center (http://www.bjmemc.com.cn/). Detailed information about sampling periods is shown in **Figure S1** and **Table S1**.

2.2. Droplet freezing assays

Total INPs, heat-sensitive INPs, lysozyme-sensitive INPs, nano-INPs (<0.22 μm) and heat-sensitive nano-INPs were determined by droplet freezing assays coupled with corresponding pretreatments with a modified instrument based on Chen et al. (2018). Five aliquots of each sample were treated separately as follows: (a) no treatment, (b) heated at 98°C for 15 min, (c) incubated with 3 mg L^{-1} lysozyme (L7773-50MG, Sigma) for 1 h at room temperature, (d) filtration through a 0.22 μm nitrous cellulose filter (Millipore, USA), (e) heated at 98°C for 15 min after treatment (d). In this study, the concentrations of INPs after no treatment and under the latter four different treatments were considered as the concentrations of total INPs, heat-resistant INPs, lysozyme-resistant INPs, nano-INPs and heat-resistant nano-INPs, respectively (Christner et al., 2008; Conen et al., 2012). The concentrations of bio-INPs and bacterial INPs were obtained by subtracting the concentrations of heat-resistant INPs and lysozyme-resistant INPs from the total INP concentrations, respectively. The concentrations of bio-nano-INPs were obtained by subtracting the concentrations of heat-resistant nano-INPs from the nano-INP concentrations.

The INA of untreated and different treated samples was determined by droplet freezing method with a modified instrument based on Chen et al. (2018). This method enables the measurement of larger particles and characterizes ice nucleation activity across a broad temperature range, making it popular for studying biological INPs. Substrate choice significantly influences the observed freezing temperature spectrum, and hydrophobic glass is commonly used as a substrate material in this method. Hydrophobic glass limits droplet spreading and contact area, and a large contact angle indicates weaker liquid-substrate interaction, which potentially reduces heterogeneous ice nucleation, enhancing experimental repeatability and accuracy. Nevertheless, hydrophobic glass may still induce ice nucleation due to micro or nanoscale surface defects. Ninety 1-μL droplets were added dropwise to a hydrophobic glass slide located on a cold stage. The cold stage was initially at 0°C and then cooled until all the droplets were frozen at a rate of 1°C min^{-1}. A charge-coupled device camera was used to record images every 6 s and the images were used to determine the freezing of droplets based on the change in grayscale values during the phase transition from liquid water to ice. As a result, the temperature and the number of frozen droplets at that temperature could be recorded. Some samples were replicated three times to ensure the accuracy of the experiment. The concentrations of INPs, bio-INPs and bacterial INPs at the freezing temperature of −18°C, and nano-INPs and biological nano-INPs at −20°C are calculated as described in previous studies (Vali, 1971) and used to perform related analysis. The laboratory (double-distilled water) and field blanks (double-distilled water poured the clean samplers before sampling) were prepared to assess the effects of contamination using the same

ice nucleation assay. The initial freezing temperature (T_0) for the laboratory blanks and filed blanks were observed to be below −20°C and −19°C, respectively. The T_0 results were comparable to the results in previous studies using a similar instrument (Chen et al., 2018) and much lower than those of samples in this study, which indicated the effect of background values using this ice nucleation assay was quite limited.

2.3. Taxonomic identification of bacteria and fungi

Samples with a volume of 50 mL were filtered by 0.22 μm polycarbonate filters (Φ 25 mm, Whatman, UK). The filters and filtrates were used for biological analysis and OM characterization, respectively. The filters were cut and placed in the lysis tubes. Subsequently, the DNA was extracted by DNeasy PowerSoil Pro Kit (Qiagen, USA) according to the manufacturer's protocol, and quantified by NanoDrop 2000 Spectrophotometers (Thermo Fischer Scientific, Inc., USA). Then a certain amount of DNA was used for polymerase chain reaction (PCR) amplification of the V3-V4 region of the 16S ribosomal RNA (rRNA) gene for bacteria and the internal transcribed spacer (ITS) region of the fungal gene. Primer pair 338F (5'-ACTCCTACGGGAGGCAGCAG-3') and 806R (5'-GGACTACHVGGGTWTCTAAT-3') for bacteria and primer pair ITS1F (5'-CTTGGTCATTTAGAGGAAGTAA-3') and ITS2 (5'-GCTGCGTTCTTCATCGATGC-3') for fungi were used for the PCR. The 20-μL PCR mixture contained 10 μL Master Mix, 0.5 μL 10 μM of each primer, 5 μL genome DNA and 4 μL double-distilled H_2O. PCR amplification was performed as follows: initial denaturation at 95°C for 5 min, followed by 35 cycles at 95°C for 30 s, 50°C for bacteria/55°C for fungi for 30 s and 72°C for 40 s, with a final elongation at 72°C for 7 min. The PCR products were purified using Agencourt AMPure XP magnetic beads. After purification, the ranges of amplified fragments and the DNA concentrations were examined using an Agilent 2100 Bioanalyzer. Then the purified PCR products were sequenced using the Illumina Hiseq 2500 platform (2×250 paired ends) at Bgi Genomics Corporation, Shenzhen, China.

The obtained reads from the platform that could match the primers have truncated the primers and connectors, and the treated reads were subjected to quality control according to the requirements of previous studies (Schmieder & Edwards, 2011). The quality-controlled reads were then stitched into tags by overlapping relationships between reads. The tags were clustered into operational taxonomic units (OTUs) at a minimum similarity of 97%. Taxonomic annotation of each OTU was performed using the Silva V138 database for bacteria and the UNITE database for fungi.

2.4. FT-ICR MS analysis and molecular formula assignment

The filtrates as mentioned in Sect. 2.3 were used to perform FT-ICR MS analysis according to previous studies (Chen et al., 2022). The Oasis hydrophilic-lipophilic balance (HLB) solid-phase extraction (SPE)-cartridges (200 mg, 6 mL) were conditioned with 3×6 mL of methanol and 2×6 mL of Milli-Q water on a Supelco Visiprep SPE Vacuum Manifold (USA). Then, samples with a volume of 50 mL were introduced at a flow rate of 1–2 mL min^{-1} onto the cartridges. A subsequent rinse of the cartridges was performed using 6 mL of Milli-Q water, after which they were dried under a nitrogen stream for 1 hour. The analytes loaded onto the cartridges were then eluted with 2×6 mL of methanol. Finally, the extracts were concentrated to 1 mL by rotary evaporators (BUCHI, Switzerland) and stored at –20°C until analysis.

The organic fractions of extracts were subjected to analysis using a 7.0T SolariX 2xR FT-ICR MS instrument (Bruker, Germany), which was equipped with an electrospray ionization source (ESI) operating in the negative ion mode. The samples were introduced into the ESI source at an infusion flow rate of 150 μL h^{-1}, with a capillary voltage set at 5000 V. Mass spectra were acquired in the range of 150 to 1000 Da, and a total of 256 scans were collected to enhance the signal-to-noise ratio (S/N) for each averaged spectrum.

Molecular formulas were assigned to mass peaks with a signal-to-noise ratio (S/N) greater than or equal to 4 using DataAnalysis v5.0 software (Bruker, Germany). The assignment of molecular formulas for the selected peaks was restricted to ^{12}C (1 − 50), ^{1}H (1 − 100), ^{16}O (1 − 30), ^{14}N (0 − 2), and ^{32}S (0 − 2). The assigned molecular formulas were categorized into four groups based on their elemental compositions: CHO, CHON, CHOS, and CHONS. The van Krevelen diagrams were used to classify molecules by H/C ratio and O/C ratio (Kim et al., 2004; Koch et al., 2007). Seven classes of compounds are distinguished according to H/C and O/C ratios: (A) lipids ($1.5 < H/C \leq 2$, $O/C \leq 0.3$), (B) aliphatic/proteins ($1.5 < H/C \leq 2.2$, $0.3 < O/C \leq 0.67$), (C) lignins/carboxylic-rich alicyclic (CRAMs)-like structures ($0.67 < H/C \leq 1.5$, $0.1 \leq O/C < 0.67$), (D) carbohydrates ($1.5 < H/C \leq 2.5$, $0.67 < O/C \leq 1.2$), (E) unsaturated hydrocarbons ($0.67 < H/C \leq 1.5$, $O/C < 0.1$), (F) aromatic structures ($0.2 \leq H/C \leq 0.67$, $O/C < 0.67$), and (G) highly oxygenated compounds (tannins) ($0.6 < H/C \leq 1.5$, $0.67 \leq O/C \leq 1.0$). More detailed information about the instrument and molecular formula assignment could be obtained from previous studies (Chen et al., 2022).

2.5. Auxiliary chemical component analyses

The subsamples were filtered with 0.22-μm pore PTFE filters (MillexGV, Millipore). The filtrates were used to analyze dissolved organic carbon (DOC) and three-dimensional excitation-emission matrix (3D-EEM). DOC was measured by using a TOC analyzer (1030 W + 1088-OI Analytical, US). Fluorescence spectra were measured using 3D-EEM fluorescence spectroscopy (Aqualog, Horiba, Japan) as described in previous studies (Fu et al., 2015).

2.6. Data analyses

Data analysis in this study was conducted using the R software (R-Core-Team, 2012). The Spearman's correlation analysis was used to assess correlations between peak area of organic molecules and INP concentrations, with a p-value less than 0.05 denoting statistical significance. Selected organic molecules with significant correlations with INPs were subjected to further analysis according to their elemental composition and classification as distinguished in the van Krevelen diagram. Co-occurrence network was constructed based on Spearman's correlation analysis. The correlation coefficients and *p*-values were calculated between organic molecules and microbial genera. P-values were adjusted to control the False Discovery Rate (FDR) using the Benjamini-Hochberg method. A network was constructed using relationships that were statistically significant ($p < 0.05$) after FDR correction. Network visualization was achieved on the interactive platform Gephi 0.10.1 (https://gephi.org/).

3. Results

3.1. Characteristics of INPs in precipitation

Figure 1 shows the cumulative spectra of total INPs per unit volume of precipitation samples collected at Mt. Lu. The concentrations of total INPs in precipitation samples were 4–4500 mL^{-1} in the temperature range from −9.6°C to −26.7°C (**Figure S1**), which were within the range of the spectra observed in rainwater over the Tibetan Plateau (Chen, Wu, Wu, et al., 2021), Quito and Mexico (Pereira et al., 2021) using the same or similar drop-freezing assays. The total INPs per unit volume of air assuming a cloud condensed water content (CWC) value of 0.4 g m^{-3} varied from 0.002 to 1.8 L^{-1} air. The T_0 for fog water and rainwater samples were from −11.2°C to −5.5°C and from −14.8°C to −9.6°C, respectively, indicating fog water had higher INA than rainwater in this study. Hartmann et al. (2021) found that fog samples collected near Canada and European Arctic contained more INPs than seawater samples, freezing onset from −15°C to −3.5°C. Previous studies observed that cloud or fog water exhibited T_0 warmer than −10°C (Gong et al., 2020; Joly et al., 2014; Schnell, 1977).

Compared to the untreated samples, heat treatment (98°C) decreased T_0 and the temperature at which 50% of the droplets frozen (T_{50}) by 2.1°C and 1.4°C on average for the rainwater samples, and by 4.2°C and 3.3°C for the fog water samples, respectively (**Table S1** and **Figure S2**). Heating treatment and lysozyme treatment are common pretreatment methods to detect biological and bacterial fractions of INPs, respectively (Christner et al., 2008; Conen et al., 2012). Results showed that heat-sensitive INPs at temperatures above −11°C constituted up to 98% of the total INPs (**Figure 2a**). On average, 33% of the INPs in fog water were lysozyme-sensitive at −11°C (**Figure 2b**). Three fog samples were completely free of lysozyme-sensitive INPs. For rainwater, half of the rainwater samples were less sensitive to lysozyme digestion throughout the freezing process. It is noted that the samples R4, R7, R8, R9 and R10 contained 11–45 heat-sensitive INPs mL^{-1} at ≥ −12°C, and almost all these INPs were susceptible to lysozyme, which suggested that bacterial INPs dominated bio-INPs in these samples.

Filtration treatment with 0.22-μm pore filters significantly reduced T_0 and T_{50} by 1.6°C and 3.0°C for the precipitation samples, respectively (**Table S1** and **Figure S2**). The INPs after filtration at −18°C in the rainwater and fog water samples accounted for 28% and 35% of the total INPs, respectively (**Figure 2c**), suggesting the considerable existence of nano-INPs (defined as INPs < 0.22 μm herein). After heat treatment of the filtrate, T_0 and T_{50} decreased by 5.1°C (6.3°C for fog water and 3.9°C for rainwater) and 3.3°C (4.9°C for fog water and 1.7°C for rainwater) on average, respectively, demonstrating the biological origin of nano-INPs, such as proteinaceous materials (Christner et al., 2008) and lipids (Hill et al., 2016).

3.2. Organic molecular compositions in precipitation

Parallel factor analysis (PARAFAC) of EEM data identified four fluorescent components (**Figure S3a**). The components C1 (240, 310/395), C2 (242, 326/452), C3 (272/321) and C4 (249, 359/445) (Ex/Em) were categorized as microbial HULIS, transitional marine HULIS, protein-like organic matter (PLOM) and terrestrial HULIS, respectively (Chen et al., 2022; Yang et al., 2019; Zhou et al., 2019). In fog water, microbial HULIS (46.1% ± 6.7%) predominated,

followed by PLOM (27.1% ± 6.2%) and terrestrial HULIS (23.9% ± 3.5%). In contrast, transitional HULIS was most prevalent in rainwater (40.8% ± 25.5%) (**Figure S3b**), highlighting distinct OM sources in rain and fog water.

FT-ICR MS analyses were performed to obtain more detailed information on OM at a molecular level, and the mass spectra of assigned chemical formulas are present in **Figure S4**. In fog and rainwater samples, 8366 and 5604 formulas were identified, respectively (**Figure S5a**). Nitrogenous compounds (CHON and CHONS) in fog water predominated, accounting for 52–69%, while the CHO and CHOS compounds accounted for 15–28% and 15–30%, respectively. The formula number of CHO and CHON compounds dominated in rainwater (67–86%), and the compounds that contained sulfur (CHOS and CHONS) occupied 25 ± 8% (**Figure S5a**). According to the nominal classification of seven compound classes in van Krevelen diagrams (Koch et al., 2007), lignins predominated among the assigned formulas in the fog and rainwater samples with a number fraction of 50% and 52%, respectively, followed by proteinaceous compounds (24% and 23%) (**Figure S5b**).

3.3. Microbial community compositions and potential taxa with INA

A total of 402 bacterial OTUs, classified into nine phyla, were detected in fog water and rainwater samples. The phyla Proteobacteria (37.7% of the total detected sequences), Firmicutes (20.8%), Actinobacteria (17.1%) and Cyanobacteria (13.7%) were the predominant phyla in all samples (**Figure S6a**). At the genus level, higher percentages of *Bacillus* (10.8%), GpI (*Anabaena*, 5.6%), and *Sphingomonas* (5.5%) were identified in rainwater samples, and the genera GpI (22.0%), and *Sphingomonas* (5.2%) dominated in fog water samples (**Figure S6b**). Genera *Pseudomonas*, *Pantoea* and *Xanthomonas*, which possibly contain potential ice nucleation-active bacterial species (Ariya et al., 2009; Kim et al., 1987; Maki et al., 1974), were detected in all samples, accounting for 3.6 ± 3.8% of the detected gene sequences (**Figure S6c**). Similar proportions of known bacteria with INA were also detected in rainwater samples from Hulunber, China (Du et al., 2017) and Kumamoto, Japan (Hu et al., 2017), and snow samples from Montreal, Canada (Mortazavi et al., 2008). Genus *Xanthomonas* was present in only six fog water and four rainwater samples, while the other two genera were detected in all samples. *Pseudomonas* accounted for 1.1 ± 1.3 and 1.7 ± 1.4% of the detected gene sequences in fog water and rainwater samples, respectively (**Figure S6c**). The relative abundance of *Pantoea* was significantly higher in rainwater samples (4.4%) than in fog water samples (0.9%).

In the fungal community, 300 OTUs were detected and classified into seven phyla. As shown in **Figure S7a**, Ascomycota (73.1%) and Basidiomycota (26.5%) emerged as the dominant phyla in all samples. In rain samples, the majority of fungi were from the genera Aspergillus (18.6%), Pseudocercospora (7.3%), and Cladosporium (5.8%) (**Figure S7b**). Among fungal community, some species of *Fusarium*, *Mortierella*, *Puccinia*, *Sarocladium* (formerly named *Acremonium*) and *Isaria* with INA could trigger ice freezing above −10°C (Fröhlich-Nowoisky et al., 2015; Haga et al., 2013; Huffman et al., 2013; Kunert et al., 2019; Pummer et al., 2015; Rodríguez Zafra et al., 2016). Of these known potential ice nucleation-active fungal genera, *Isaria*, *Sarocladium*, *Fusarium* and *Mortierella* were detectable in some samples, with a fraction of 0.006%, 0.38%, 0.37% and 0.007% on average, respectively. Known ice nucleation-active fungal species *Sarocladium implicatum* were detected in more than half of the samples (**Figure S7c**). However, the total abundances of known potential ice nucleation-active fungal genera

detected in this study were minor (0.6 ± 1.3%), indicating the possible existence of unknown ice nucleation-active microbial taxa.

3.4. Relationship between INPs and OM compositions in precipitation

Spearman's correlation revealed that PLOM (C3) and terrestrial HULIS (C4) were significantly positively related with total, heat-sensitive, and lysozyme-sensitive INPs at –18°C, and nano-INPs and heat-sensitive nano-INPs at –20°C (**Figure S8**). However, transitional marine HULIS (C2) exhibited a strong negative correlation with INPs, suggesting potential interference in INP formation by certain substances. To deepen the understanding of the relationship between OM at a molecular level and INPs, we conducted Spearman's correlation analysis of the detected organic formula peak intensities and different types of INP concentrations. The analysis revealed significant correlations ($p < 0.05$) for 2926, 2108 and 1382 formulas with total, heat-sensitive, and lysozyme-sensitive INPs at –18°C, respectively (**Figure S9**). Among these INP-related formulas, the CHONS group was predominant (34–48%), followed by the CHOS group (30–36%) (**Figure S9a**). OM molecules significantly correlated with different types of INPs are illustrated by van Krevelen diagrams to facilitate the classification of INP-related OM molecules (**Figure 3**), and results showed that the INP-related formulas were mainly assigned to proteinaceous compounds (38–43%) and lignins (28–35%).

After filtration treatment, more OM molecules were associated with the concentrations of nano-INPs (formula number: 5380) and heat-sensitive nano-INPs at –20°C (formula number: 5379) (**Figure S9**), which were dominated by CHONS compounds with a fraction of 56%. According to the compound classes, these formulas were mainly assigned to lignins, accounting for 38%, followed by proteinaceous compounds (37%). When correlation coefficients exceeded 0.7, the majority of formulas linked to total, heat-sensitive, and lysozyme-sensitive INPs were proteinaceous compounds (67%, 71% and 72%, respectively) and carbohydrates (17%, 15% and 17%). For nano-INPs and heat-sensitive nano-INPs, proteinaceous substances predominated, accounting for 59% and 54% respectively (**Figure S10**).

3.5. Relations between microbial taxa and biological INPs-related organic molecules

To ascertain if microorganisms contribute organic molecules that potentially affect INPs, we conducted a co-occurrence network analysis based on Spearman's correlations analysis between microbial communities (including bacteria and fungi) and the organic molecules significantly associated with heat-sensitive INPs (r values > 0.7, formula number: 64) (**Figure S11**). In the constructed network, nodes symbolize OM and microbial genera, and edges denote the correlation strength between OM and microbial genera. A total of 197 and 500 pairs of correlations were established between bacterial and fungal genera and these organic formulas, respectively (**Figure S11**). Twelve bacterial and 13 fungal genera were linked to the organic formulas. Bacterial genera GpI (*Anabaena*), *Friedmanniella* and *Roseomonas* exhibited the highest degree centrality values of 26.5%, 29.1%, and 18.3%, respectively, indicating more organic molecule associations. *Paenibacillus*, *Romboutsia* and *Clostridium_sensu_stricto 1* showed negative associations with some carbohydrate molecules. Other bacterial genera had limited associations with organic molecules. Meanwhile, strong correlations between 13 fungal genera and organic molecules were noted (**Figure S11**). *Sistotrema*, *Hydnomerulius*, *Stereum*, *Diatrype*, *Pseudocercospora* and *Neocucurbitaria* were closely linked together and

predominated in all relationships. Moreover, *Trametes* and *Hypholoma* also exhibited positive correlations with the organic molecules, while *Herpotrichia* showed negative interactions.

The network between microbial taxa and biological nano-INPs-related OM formulas (r values > 0.7, formula number: 507) revealed that 18 bacterial and 17 fungal genera interacted with the OM formulas, including all genera found in the previous network (**Figure 4**). The resulting network was composed of 525 nodes and 1486 edges for bacteria, and 469 nodes and 1259 edges for fungi, respectively. Predominant bacterial genera in the network were *Microbacterium*, GpI, *Acidisphaera* and *Roseomonas*, mainly associated with proteinaceous compounds and lipids. In contrast, several Ascomycota phylum members like *Neocucurbitaria*, *Pseudocercospora*, *Cadophora*, and *Herpotrichia* showed negative associations with proteinaceous compounds and lipids, while Basidiomycota phylum members *Hydnomerulius* and *Sistotrema* displayed strong positive correlations with these compounds.

4. Discussion

4.1. Dominant contribution of biological matters to precipitation INPs

The INPs in all rainwater samples initiated freezing at temperatures above −15°C, and nearly all fog water samples contained INPs active at ≥ −10 °C (**Figure 1**). High T_0 and T_{50} values often signify bio-INPs presence, as many known bio-INPs trigger ice formation at temperatures above −15°C, while the ice nucleation-active at < −15°C is typically dominated by minerals (Hiranuma et al., 2013; Hoose & Möhler, 2012; Murray et al., 2013). Here, heat-sensitive INPs represented bio-INPs (Conen et al., 2022; Sze et al., 2023; Tang et al., 2022), as heating treatment can reduce the INA of many biological materials (e.g., bacteria, fungi, leaf debris) by inactivating ice nucleation proteinaceous matter (Failor et al., 2017; Hill et al., 2016; Pouleur et al., 1992; Schnell & Vali, 1973), though certain pollen is heat-resistant to temperature > 95°C (Duan et al., 2023; Pummer et al., 2012).

Results showed that the total INPs in all the rainwater samples initiated freezing at temperatures warmer than −15°C, and almost all the fog water samples contained INPs active at ≥ −10°C (**Figure 1**). The mechanisms of fog and rain formation differ, as well as the conditions and physical processes under which they exist in the atmosphere. The formation of fog primarily occurs through the direct condensation of water vapor onto ice nuclei or condensation nuclei, resulting in the formation of tiny water droplets (Gill et al., 1983; Gultepe et al., 2007), which may cause INPs to be more concentrated within the fog. In contrast, rain formation involves different atmospheric processes and conditions that might not always enhance the INP concentrations as much as in fog. Additionally, fog droplets are smaller, providing a larger surface area capable of more effectively absorbing and enriching particulate matter in the air. Compared to rainwater, the limited dilution of fog water and the more efficient transfer of surface emissions to fog water may contribute to higher concentrations of particulate matter in fog water (Klemm & Wrzesinsky, 2007). The total INPs at temperatures > −15°C in fog water contained a large fraction (51.2%) of heat-sensitive INPs, with proportions increasing with temperature in most samples (**Figure 2**), suggesting a dominance of biological materials in INPs. The bio-INPs to non-bio-INPs ratio was significantly higher in fog water (10.5%) than in rainwater (1.6%), indicating a greater contribution of bio-INPs in fog water. Notably, fractions of heat-sensitive INPs at −24°C to −20°C enhanced to 78% and 89% on average in R6 and R7,

respectively, indicating other INP types besides bio-INPs (Atkinson et al., 2013; Hiranuma et al., 2013), also found by Chen, Wu, Chen, et al. (2021). Some inorganic substances (e.g., quartz) whose INA is reduced by thermal interference, and other non-thermally labile substances may contribute to this phenomenon (Harrison et al., 2019; Wilson et al., 2015).

Bacteria are potentially an important type of bio-INPs considering their number in air (Failor et al., 2017; Lohmann & Feichter, 2005; Morris et al., 2004). INPs sensitive to lysozyme digestion (i.e., to dissolve the cell wall structure) have been widely regarded as bacterial INPs (Christner et al., 2008; Failor et al., 2017; Morris et al., 2013). However, lysozyme mainly acts on peptidoglycans (Masschalck & Michiels, 2003; Repaske, 1956), less effective on Gram-negative bacteria with low peptidoglycan cell wall content (Joly et al., 2014), and the INA of urediospores of rust fungi even increased after lysozyme treatment (Morris et al., 2013). Therefore, the use of lysozyme-sensitive INPs to indicate bacterial INPs may be subject to some error. Lysozyme-sensitive INPs accounted for 44.8% of bio-INPs, suggesting other types of biological particles, e.g., Gram-negative bacteria, fungi, or plant debris also contributed to bio-INPs.

The filtration tests showed a certain number of INPs passed through 0.2 μm filters (**Figure S2**), suggesting the existence of nano-INPs. Nanoscale INPs could promote the efficient formation of ice embryos due to the large specific surface area (Pruppacher & Klett, 2010) or attachment to the particle surfaces thereby enhancing the INA of particles (O'Sullivan et al., 2016; Pummer et al., 2015). Such findings were observed in terrestrial and marine ecosystems (Augustin et al., 2013; Du et al., 2017) and nano-INPs were highly likely contributed by smaller biological particles (Pummer et al., 2015). Known ice nucleation-active bacteria or fungi could exist as submicron fragments, and microbial fragments and ice nucleation-active proteinaceous matter were passed through the filter and retained in the filtrate (Šantl-Temkiv et al., 2015). Pollen readily released large amounts of nanoscale INPs when in contact with water (Augustin et al., 2013; Duan et al., 2023). This was consistent with the finding in this study that the proportions of nano-INPs in total INPs were almost identical to that of heat-sensitive nano-INPs (**Figure 2**). These nano-INPs were mainly biological, such as proteinaceous materials, lipid bodies, carbohydrates and cell structures (such as ribosomes), which could be degraded or inactivated by heating (Hill et al., 2016; Rederstorff et al., 2011; Urano & Douple, 2023).

4.2. OM molecules with high INA in precipitation

Figure 3 depicts sulfur-containing compounds (CHOS, CHONS) dominating the OM formulas associated with INPs, with a positive correlation between different INP concentrations and the formula numbers of CHOS and CHONS (**Table S2**), highlighting the possible importance of sulfur-containing compounds in INPs. Previous studies have demonstrated that under deposition nucleation mode sulfate-organic particles could promote heterogeneous ice nucleation (Froyd et al., 2010; Knopf et al., 2018), and organosulfur compounds dominated ice residuals (Cziczo et al., 2013; DeMott et al., 2003). Several potential explanations were proposed in previous studies regarding OM molecules as INPs. Fukuta (1966) proposed that organics with INA are mostly crystalline solids with low solubility and high melting points, having polar or hydrogen bonding groups as active sites. Baustian et al. (2012) uncovered a complex link between ice formation and organic materials, with INA potentially influenced by chemical composition and spatial chemical arrangement in mixed particles. Here, CHOS and CHONS were predominantly assigned to proteinaceous compounds (**Figure 3**), possibly vital for ice formation (O'Sullivan et

al., 2016; Šantl-Temkiv et al., 2019), partially accounting for the possible INA of the sulfur-containing compounds in this study. Several possible structures of these proteinaceous compounds are presented in **Figure 3f**. Due to technical limitations, only the molecular formulas and the classification of the detected compounds could be identified, and the molecular structures are not yet known due to isomers. The proteinaceous compounds shown in **Figure 3f** represent merely one among several potential structures. The precise molecular structures, as yet undetermined, necessitate additional comprehensive investigation.

Proteinaceous materials are the most studied organics to nucleate ice because the presence of proteinaceous matter in the outer layer of the cell membrane enables the INA of microorganisms (Gurian-Sherman & Lindow, 1993; Lindow et al., 1989). The structure of ice nucleation-active proteinaceous matter contains a hydrophobic N-terminal domain, a hydrophilic C-terminal domain and a large central repeating domain that can act as an ice nucleation site (Huang et al., 2021; Wolber & Warren, 1989). In this study, more proteinaceous compounds had positive relationships with different types of INPs (**Figure 3**), further clarifying the important contribution of proteinaceous matter to INPs. Interestingly, some proteinaceous compounds exhibiting negative correlations with INPs were identified (**Figure 3** and **Table S3**), implying the presence of antifreeze proteinaceous materials (Davies, 2014; Dreischmeier et al., 2017; Govindarajan & Lindow, 1988). These proteinaceous materials are ice-structured materials that inhibit ice growth by maintaining the temperature in the range between the melting point and the freezing point(Baskaran et al., 2021).

In addition, lignins and carbohydrates were also significantly positively correlated with INPs (**Figure 3** and **S9**). Lignin-like substances are complex organic polymers derived from the cell wall structure of vascular plants (Miller et al., 2021). A large number of lignins existing in plant xylem had INA (Conen et al., 2016; Gute & Abbatt, 2020), and lignins have been identified as water-soluble macromolecules with INA (Pummer et al., 2015; Steinke et al., 2020). The INA of lignins may also be confirmed by the result that more lignin molecules were highly related to nano-INPs compared to total INPs (**Figure S9**). In addition, due to the stable INA under different environmental stresses (Bogler & Borduas-Dedekind, 2020), lignins have been recommended for use as an ice-nucleating standard (Miller et al., 2021).

Carbohydrates largely contributed to the INA of pollen or plants (Dreischmeier et al., 2017; Krog et al., 1979). Carbohydrate mixtures with other substances (e.g., mucilage or proteinaceous substances) serve as intrinsic ice nucleators in some plants (Brush et al., 1994; Embuscado et al., 1996). Under high humidity, pollen emits vast amounts of carbohydrate-rich submicron particles that retain the INA of the parent body (Duan et al., 2023; Hill et al., 2017; Pummer et al., 2012; Steiner et al., 2015). Notably, some polysaccharides can inhibit ice nucleation (Yamashita et al., 2002), with their effect on ice formation depending on molecular size and structure (Dreischmeier et al., 2017; Duan et al., 2023; Walters et al., 2009). Dreischmeier et al. (2017) found that the smaller polysaccharides (< 100 kDa) exhibited stronger ice-binding abilities. The molecular structure of known INPs shows that INA is primarily attributed to the presence of hydroxyl groups in the molecules (Graether & Jia, 2001), which could potentially elucidate the INA of carbohydrates with multiple hydrogen bonds, especially those with hydroxyl groups (Wolf et al., 2019).

4.3. Potential microbial sources of INPs-related OM molecules

Fundamentally, microorganisms own INA because of the presence of intrinsic substances that promote ice nucleation (Delort et al., 2010). These substances are likely to be biological macromolecules such as proteinaceous substances, lipids and carbohydrates (Koop & Zobrist, 2009). Ice-nucleating sites in bacteria and fungi were mainly contributed by proteinaceous substances, while pollen is more likely to be contributed by carbohydrates and/or proteinaceous substances (Dreischmeier et al., 2017; O'Sullivan et al., 2016). This is in agreement with the findings in this study that proteinaceous or carbohydrate-like substances significantly correlated with INPs (**Figure 3**). In the constructed co-occurrence networks, bacterial taxa with positive correlations with OMs mostly belong to the order Actinomycetales (**Figure S12**) which are filamentous Gram-positive bacteria without a nucleus (Yanti et al., 2012). The known ice-nucleating bacteria were mostly Gram-negative (Maki et al., 1974), but a few Gram-positive species with INA were also detected (Failor et al., 2017). Recent studies isolated several Gram-positive bacteria with INA, i.e., *Paenibacillus* sp., *Bacillus* sp. (Beall et al., 2021), and some species of Actinomycetes (such as *Microbacterium esteraromaticum*, *Rhodococcus corynebacteroide* and *Brevibacterium* sp.)(Cid et al., 2016), some of which were also occurred in the constructed co-occurrence networks.

Compared with bacteria (edges: 772), fungi (edges: 492) were positively associated with fewer nano-INPs-related OM molecules (**Figure 4**), suggesting a lesser contribution of fungi to nano-INPs-related OM molecules. In previous studies, fungi with high INA were some lichen mycobionts (Kieft & Ruscetti, 1990) and some species of *Fusarium*, *Penicillium* and *Cladosporium* (Pouleur et al., 1992). Recently, ice nucleation abilities were detected in other fungal taxa, e.g., some species of *Isaria* and *Acremonium* (Huffman et al., 2013), as well as in some rust fungi (Morris et al., 2013). Among them, rust fungi had a high capacity for ice nucleation, which initiated ice nucleation at > −4°C (Morris et al., 2013), but most fungi were less capable of ice formation than bacteria (Maki et al., 1974; Obata et al., 1989). Meanwhile, the genera positively associated with nano-INPs-related OM molecules were *Hydnomerulius* and *Sistotrema*, which belong to Agaricomycetes, implying a potential ice nucleation ability of Agaricomycetes. A similar finding was provided by Tang et al. (2022) that elevated INP concentrations in precipitation were accompanied by increases in the relative abundances of Agaricomycetes.

The presence of proteins, carbohydrates or lipid fractions with ice nucleation or antifreeze capabilities within the microorganism enable diverse biological entities to influence ice formation differently (Dreischmeier et al., 2017; O′Sullivan et al., 2015). Nonetheless, OM molecules were significantly smaller than intact cells (Govindarajan & Lindow, 1988; Pummer et al., 2012), and the possibility of organic compounds with varying ice nucleation abilities coexisting within the same microorganism cannot be discounted (Dreischmeier et al., 2017; Failor et al., 2017; Rice et al., 2015). Certain proteinaceous materials or carbohydrates possess both ice-binding and ice-nucleating abilities (Xu et al., 1998). For example, the large ice-nucleating polysaccharides in birch pollen may be composed of smaller clusters of ice-binding polysaccharides (Dreischmeier et al., 2017). Moreover, a fraction of the ice-nucleating protein within *Pseudomonas syringae* exhibited ice-binding capability (Kobashigawa et al., 2005). This mechanism could help explain the occurrence of a comparable microbial taxa in both co-

occurrence networks of bio-INPs-related and biological nano-INPs-related OM formulas with microbial communities (**Figure 4 and S11**).

5. Conclusions

Building upon previous research works, this study for the first time emphasizes the linkage between INPs, organic molecules, and microorganisms in environmental precipitation samples. It highlights the significant contribution of biological materials to INPs, advancing our understanding of these interactions in real environments. OM molecules associated with INPs predominantly comprised sulfur-containing compounds, as revealed by the van Krevelen diagram, which allocated these molecules chiefly to biologically relevant categories such as proteins, lignin, and carbohydrates. Co-occurrence networks further corroborated that specific microorganisms may contribute to INP-related OM molecules, with the contribution from bacteria being more substantial than that from fungi. It warrants acknowledgment, however, that the genera appearing in co-occurrence networks have not been tested for INA, and the known ice-nucleating taxa did not feature in the networks. The ice nucleation capacity of a considerable array of microbial taxa remains uncharted owing to microbial diversity, and the studies scrutinizing OM molecules possessing INA in organisms are still limited. Future investigations are imperative for the identification of the ice nucleation ability across a broader spectrum of microbial taxa.

Acknowledgments

This work was supported by the National Key R&D Plan (Grant No. 2022YFF0803000).

Conflict of Interest

The authors declare no conflicts of interest relevant to this study.

Data Availability Statement

The sequences have been deposited in the NCBI with BioProject accession number PRJNA994904 (https://www.ncbi.nlm.nih.gov/sra/PRJNA994904). Detailed methods in the study are available in the supporting information. The data are hosted at https://zenodo.org/records/10300240 (Niu et al., 2024).

References

Ahern, H. E., Walsh, K. A., Hill, T. C. J., & Moffett, B. F. (2007). Fluorescent pseudomonads isolated from Hebridean cloud and rain water produce biosurfactants but do not cause ice nucleation. *Biogeosciences, 4*(1), 115-124. https://doi.org/10.5194/bg-4-115-2007

Ariya, P. A., Sun, J., Eltouny, N. A., Hudson, E. D., Hayes, C. T., & Kos, G. (2009). Physical and chemical characterization of bioaerosols – Implications for nucleation processes. *International Reviews in Physical Chemistry, 28*(1), 1-32. 10.1080/01442350802597438

Arny, D., Lindow, S., & Upper, C. (1976). Frost sensitivity of Zea mays increased by application of *Pseudomonas syringae*. *Nature, 262*, 282–284. https://doi.org/10.1038/262282a0

Atkinson, J. D., Murray, B. J., Woodhouse, M. T., Whale, T. F., Baustian, K. J., Carslaw, K. S., et al. (2013). The importance of feldspar for ice nucleation by mineral dust in mixed-phase clouds. *Nature, 498*(7454), 355-358. https://doi.org/10.1038/nature12278

Augustin, S., Wex, H., Niedermeier, D., Pummer, B., Grothe, H., Hartmann, S., et al. (2013). Immersion freezing of birch pollen washing water. *Atmospheric Chemistry & Physics, 13*(21), 10989-11003. https://doi.org/10.5194/acp-13-10989-2013

Baskaran, A., Kaari, M., Venugopal, G., Manikkam, R., Joseph, J., & Bhaskar, P. V. (2021). Anti freeze proteins (Afp): Properties, sources and applications – A review. *International Journal of Biological Macromolecules, 189*, 292-305. https://doi.org/10.1016/j.ijbiomac.2021.08.105

Baustian, K. J., Cziczo, D. J., Wise, M. E., Pratt, K. A., Kulkarni, G., Hallar, A. G., & Tolbert, M. A. (2012). Importance of aerosol composition, mixing state, and morphology for heterogeneous ice nucleation: A combined field and laboratory approach. *Journal of Geophysical Research: Atmospheres, 117*(D6), D06217. https://doi.org/10.1029/2011JD016784

Beall, C. M., Lucero, D., Hill, T. C., DeMott, P. J., Stokes, M. D., & Prather, K. A. (2020). Best practices for precipitation sample storage for offline studies of ice nucleation in marine and coastal environments. *Atmospheric Measurement Techniques, 13*(12), 6473-6486. https://doi.org/10.5194/amt-13-6473-2020

Beall, C. M., Michaud, J. M., Fish, M. A., Dinasquet, J., Cornwell, G. C., Stokes, M. D., et al. (2021). Cultivable halotolerant ice-nucleating bacteria and fungi in coastal precipitation. *Atmospheric Chemistry & Physics, 21*(11), 9031-9045. https://doi.org/10.5194/acp-21-9031-2021

Bogler, S., & Borduas-Dedekind, N. (2020). Lignin's ability to nucleate ice via immersion freezing and its stability towards physicochemical treatments and atmospheric processing. *Atmospheric Chemistry & Physics, 20*(23), 14509-14522. https://doi.org/10.5194/acp-20-14509-2020

Borduas-Dedekind, N., Ossola, R., David, R. O., Boynton, L. S., Weichlinger, V., Kanji, Z. A., & McNeill, K. (2019). Photomineralization mechanism changes the ability of dissolved organic matter to activate cloud droplets and to nucleate ice crystals. *Atmospheric Chemistry & Physics, 19*(19), 12397-12412. https://doi.org/10.5194/acp-19-12397-2019

Brush, R. A., Griffith, M., & Mlynarz, A. (1994). Characterization and quantification of intrinsic ice nucleators in winter rye (*Secale cereale*) leaves. *Plant Physiology, 104*(2), 725-735. https://doi.org/10.1104/pp.104.2.725

Cascajo-Castresana, M., David, R. O., Iriarte-Alonso, M. A., Bittner, A. M., & Marcolli, C. (2020). Protein aggregates nucleate ice: The example of apoferritin. *Atmospheric Chemistry & Physics, 20*(6), 3291-3315. https://doi.org/10.5194/acp-20-3291-2020

Che, Y., Dang, J., Fang, W., Shen, X., Sun, J., Chen, Y., & Qian, Y. (2019). Measurements of natural ice nucleating particles in Beijing in the spring of 2017. *Atmospheric Environment, 200*, 170-177. https://doi.org/10.1016/j.atmosenv.2018.12.020

Chen, J., Pei, X. Y., Wang, H., Chen, J. C., Zhu, Y. S., Tang, M. G., & Wu, Z. J. (2018). Development, characterization, and validation of a cold stage-based ice nucleation array (PKU-INA). *Atmosphere, 9*(9), 357. https://doi.org/10.3390/atmos9090357

Chen, J., Wu, Z., Chen, J., Reicher, N., Fang, X., Rudich, Y., & Hu, M. (2021). Size-resolved atmospheric ice-nucleating particles during East Asian dust events. *Atmospheric Chemistry & Physics, 21*(5), 3491-3506. https://doi.org/10.5194/acp-21-3491-2021

Chen, J., Wu, Z. J., Wu, G. M., Gong, X. D., Wang, F., Chen, J. C., et al. (2021). Ice-nucleating particle concentrations and sources in rainwater over the third pole, Tibetan Plateau. *Journal of Geophysical Research: Atmospheres, 126*(9), e2020JD033864. https://doi.org/10.1029/2020JD033864

Chen, J., Wu, Z. J., Zhao, X., Wang, Y. J., Chen, J. C., Qiu, Y. T., et al. (2021). Atmospheric humic-like substances (HULIS) act as ice active entities. *Geophysical Research Letters, 48*(14), e2021GL092443. https://doi.org/10.1029/2021GL092443

Chen, S., Xie, Q., Su, S., Wu, L., Zhong, S., Zhang, Z., et al. (2022). Source and formation process impact the chemodiversity of rainwater dissolved organic matter along the Yangtze River Basin in summer. *Water Research, 211*, 118024. https://doi.org/10.1016/j.watres.2021.118024

Christner, B. C. (2010). Bioprospecting for microbial products that affect ice crystal formation and growth. *Applied Microbiology and Biotechnology, 85*(3), 481-489. https://doi.org/10.1007/s00253-009-2291-2

Christner, B. C., Cai, R., Morris, C. E., McCarter, K. S., Foreman, C. M., Skidmore, M. L., et al. (2008). Geographic, seasonal, and precipitation chemistry influence on the abundance and activity of biological ice nucleators in rain and snow. *The Proceedings of the National Academy of Sciences, 105*(48), 18854-18859. https://doi.org/10.1073/pnas.0809816105

Cid, F. P., Rilling, J. I., Graether, S. P., Bravo, L. A., Mora, M. d. L. L., & Jorquera, M. A. (2016). Properties and biotechnological applications of ice-binding proteins in bacteria. *FEMS Microbiology Letters, 363*(11), fnw099. https://doi.org/10.1093/femsle/fnw099

Conen, F., Einbock, A., Mignani, C., & Hüglin, C. (2022). Measurement report: Ice-nucleating particles active ≥ −15°C in free tropospheric air over western Europe. *Atmospheric Chemistry & Physics, 22*(5), 3433-3444. https://doi.org/10.5194/acp-22-3433-2022

Conen, F., Henne, S., Morris, C. E., & Alewell, C. (2012). Atmospheric ice nucleators active ≥ −12 °C can be quantified on PM_{10} filters. *Atmospheric Measurement Techniques, 5*(2), 321-327. https://doi.org/10.5194/amt-5-321-2012

Conen, F., Morris, C. E., Leifeld, J., Yakutin, M. V., & Alewell, C. (2011). Biological residues define the ice nucleation properties of soil dust. *Atmospheric Chemistry & Physics, 11*(18), 9643-9648. https://doi.org/10.5194/acp-11-9643-2011

Conen, F., Rodríguez, S., Hülin, C., Henne, S., Herrmann, E., Bukowiecki, N., & Alewell, C. (2015). Atmospheric ice nuclei at the high-altitude observatory Jungfraujoch, Switzerland. *Tellus B: Chemical and Physical Meteorology, 67*(1), 25014. https://doi.org/10.3402/tellusb.v67.25014

Conen, F., Stopelli, E., & Zimmermann, L. (2016). Clues that decaying leaves enrich Arctic air with ice nucleating particles. *Atmospheric Environment, 129*, 91-94. https://doi.org/10.1016/j.atmosenv.2016.01.027

Creamean, J. M., Lee, C., Hill, T. C., Ault, A. P., DeMott, P. J., White, A. B., et al. (2014). Chemical properties of insoluble precipitation residue particles. *Journal of Aerosol Science, 76*, 13-27. https://doi.org/10.1016/j.jaerosci.2014.05.005

Creamean, J. M., Mignani, C., Bukowiecki, N., & Conen, F. (2019). Using freezing spectra characteristics to identify ice-nucleating particle populations during the winter in the Alps. *Atmospheric Chemistry & Physics, 19*(12), 8123-8140. https://doi.org/10.5194/acp-19-8123-2019

Creamean, J. M., Suski, K. J., Rosenfeld, D., Cazorla, A., DeMott, P. J., Sullivan, R. C., et al. (2013). Dust and Biological Aerosols from the Sahara and Asia Influence Precipitation in the Western U.S. *Science, 339*(6127), 1572-1578. https://doi.org/10.1126/science.1227279

Creamean, J. M., White, A. B., Minnis, P., Palikonda, R., Spangenberg, D. A., & Prather, K. A. (2016). The relationships between insoluble precipitation residues, clouds, and precipitation over California's southern Sierra Nevada during winter storms. *Atmospheric Environment, 140*, 298-310. https://doi.org/10.1016/j.atmosenv.2016.06.016

Cziczo, D. J., Froyd, K. D., Hoose, C., Jensen, E. J., Diao, M., Zondlo, M. A., et al. (2013). Clarifying the dominant sources and mechanisms of cirrus cloud formation. *Science, 340*(6138), 1320-1324. https://doi.org/10.1126/science.1234145

Davies, P. L. (2014). Ice-binding proteins: a remarkable diversity of structures for stopping and starting ice growth. *Trends in Biochemical Sciences, 39*(11), 548-555. https://doi.org/10.1016/j.tibs.2014.09.005

Delort, A.-M., Vaïtilingom, M., Amato, P., Sancelme, M., Parazols, M., Mailhot, G., et al. (2010). A short overview of the microbial population in clouds: Potential roles in atmospheric chemistry and nucleation processes. *Atmospheric Research, 98*(2), 249-260. https://doi.org/10.1016/j.atmosres.2010.07.004

DeMott, P. J., Cziczo, D. J., Prenni, A. J., Murphy, D. M., Kreidenweis, S. M., Thomson, D. S., et al. (2003). Measurements of the concentration and composition of nuclei for cirrus formation. *The Proceedings of the National Academy of Sciences, 100*(25), 14655-14660. https://doi.org/10.1073/pnas.2532677100

DeMott, P. J., Prenni, A. J., Liu, X., Kreidenweis, S. M., Petters, M. D., Twohy, C. H., et al. (2010). Predicting global atmospheric ice nuclei distributions and their impacts on climate. *The Proceedings of the National Academy of Sciences, 107*(25), 11217-11222. https://doi.org/10.1073/pnas.0910818107

Dreischmeier, K., Budke, C., Wiehemeier, L., Kottke, T., & Koop, T. (2017). Boreal pollen contain ice-nucleating as well as ice-binding 'antifreeze' polysaccharides. *Scientific Reports, 7*(1), 41890. https://doi.org/10.1038/srep41890

Du, R., Du, P., Lu, Z., Ren, W., Liang, Z., Qin, S., et al. (2017). Evidence for a missing source of efficient ice nuclei. *Scientific Reports, 7*(1), 39673. https://doi.org/10.1038/srep39673

Duan, P., Hu, W., Wu, Z., Bi, K., Zhu, J., & Fu, P. (2023). Ice nucleation activity of airborne pollen: A short review of results from laboratory experiments. *Atmospheric Research, 285*, 106659. https://doi.org/10.1016/j.atmosres.2023.106659

Embuscado, M. E., BeMiller, J. N., & Knox, E. B. (1996). A survey and partial characterization of iceucleating fluids secreted by giant-rosette (*Lobelia* and *Dendrosenecio*) plants of the mountains of eastern Africa. *Carbohydrate Polymers, 31*(1), 1-9. https://doi.org/10.1016/S0144-8617(96)00120-8

Failor, K. C., Liu, H., Llontop, M. E. M., LeBlanc, S., Eckshtain-Levi, N., Sharma, P., et al. (2022). Ice nucleation in a Gram-positive bacterium isolated from precipitation depends on a polyketide synthase and non-ribosomal peptide synthetase. *The ISME Journal, 16*(3), 890-897. https://doi.org/10.1038/s41396-021-01140-4

Failor, K. C., Schmale, D. G., Vinatzer, B. A., & Monteil, C. L. (2017). Ice nucleation active bacteria in precipitation are genetically diverse and nucleate ice by employing different mechanisms. *The ISME Journal, 11*(12), 2740-2753. https://doi.org/10.1038/ismej.2017.124

Fröhlich-Nowoisky, J., Hill, T. C. J., Pummer, B. G., Yordanova, P., Franc, G. D., & Pöschl, U. (2015). Ice nucleation activity in the widespread soil fungus *Mortierella alpina*. *Biogeosciences, 12*(4), 1057-1071. https://doi.org/10.5194/bg-12-1057-2015

Froyd, K. D., Murphy, D. M., Lawson, P., Baumgardner, D., & Herman, R. L. (2010). Aerosols that form subvisible cirrus at the tropical tropopause. *Atmospheric Chemistry & Physics, 10*(1), 209-218. https://doi.org/10.5194/acp-10-209-2010

Fu, P., Kawamura, K., Chen, J., Qin, M., Ren, L., Sun, Y., et al. (2015). Fluorescent water-soluble organic aerosols in the High Arctic atmosphere. *Scientific Reports, 5*(1), 9845. https://doi.org/10.1038/srep09845

Fukuta, N. (1966). Experimental studies of organic ice nuclei. *Journal of Atmospheric Sciences, 23*(2), 191-196. https://doi.org/10.1175/1520-0469(1966)023<0191:ESOOIN>2.0.CO;2

Gill, P. S., Graedel, T. E., & Weschler, C. J. (1983). Organic films on atmospheric aerosol particles, fog droplets, cloud droplets, raindrops, and snowflakes. *Reviews of Geophysics, 21*(4), 903-920. https://doi.org/10.1029/RG021i004p00903

Gong, X., Wex, H., Voigtländer, J., Fomba, K. W., Weinhold, K., van Pinxteren, M., et al. (2020). Characterization of aerosol particles at Cabo Verde close to sea level and at the cloud level – Part 1: Particle number size distribution, cloud condensation nuclei and their origins. *Atmospheric Chemistry & Physics, 20*(3), 1431-1449. https://doi.org/10.5194/acp-20-1431-2020

Govindarajan, A. G., & Lindow, S. E. (1988). Size of bacterial ice-nucleation sites measured in situ by radiation inactivation analysis. *Proceedings of the National Academy of Sciences, 85*(5), 1334-1338. https://doi.org/10.1073/pnas.85.5.1334

Graether, S. P., & Jia, Z. (2001). Modeling *Pseudomonas syringae* ice-nucleation protein as a β-helical protein. *Biophysical Journal, 80*(3), 1169-1173. https://doi.org/10.1016/S0006-3495(01)76093-6

Gultepe, I., Tardif, R., Michaelides, S. C., Cermak, J., Bott, A., Bendix, J., et al. (2007). Fog Research: A Review of Past Achievements and Future Perspectives. *Pure and Applied Geophysics, 164*(6), 1121-1159. https://doi.org/10.1007/s00024-007-0211-x

Guo, L., Guo, X., Lou, X., Lu, G., Lü, K., Sun, H., et al. (2019). An observational study of diurnal and seasonal variations, and macroscopic and microphysical properties of clouds and precipitation over Mount Lu, Jiangxi, China. *Acta Meteorologica Sinica, 77*(5), 923-937. https://doi.org/10.11676/qxxb2019.056

Gurian-Sherman, D., & Lindow, S. E. (1993). Bacterial ice nucleation: Significance and molecular basis. *FASEB Journal, 7*(14), 1338-1343. https://doi.org/10.1096/fasebj.7.14.8224607

Gute, E., & Abbatt, J. P. D. (2020). Ice nucleating behavior of different tree pollen in the immersion mode. *Atmospheric Environment, 231*, 117488. https://doi.org/10.1016/j.atmosenv.2020.117488

Haga, D. I., Iannone, R., Wheeler, M. J., Mason, R., Polishchuk, E. A., Fetch Jr., T., et al. (2013). Ice nucleation properties of rust and bunt fungal spores and their transport to high altitudes, where they can cause heterogeneous freezing. *Journal of Geophysical Research: Atmospheres, 118*(13), 7260-7272. https://doi.org/10.1002/jgrd.50556

Harrison, A. D., Lever, K., Sanchez-Marroquin, A., Holden, M. A., Whale, T. F., Tarn, M. D., et al. (2019). The ice-nucleating ability of quartz immersed in water and its atmospheric importance compared to K-feldspar. *Atmospheric Chemistry & Physics, 19*(17), 11343-11361. https://doi.org/10.5194/acp-19-11343-2019

Hartmann, M., Gong, X., Kecorius, S., van Pinxteren, M., Vogl, T., Welti, A., et al. (2021). Terrestrial or marine – indications towards the origin of ice-nucleating particles during melt season in the European Arctic up to 83.7°N. *Atmospheric Chemistry & Physics, 21*(15), 11613-11636. https://doi.org/10.5194/acp-21-11613-2021

Hew, C. L., & Yang, D. S. (1992). Protein interaction with ice. *European Journal of Biochemistry, 203*(1-2), 33-42. https://doi.org/10.1111/j.1432-1033.1992.tb19824.x

Hill, T. C. J., DeMott, P. J., Conen, F., & Möhler, O. (2017). Impacts of bioaerosols on atmospheric ice nucleation processes. In *Microbiology of Aerosols* (pp. 195-219).

Hill, T. C. J., DeMott, P. J., Tobo, Y., Fröhlich-Nowoisky, J., Moffett, B. F., Franc, G. D., & Kreidenweis, S. M. (2016). Sources of organic ice nucleating particles in soils. *Atmospheric Chemistry & Physics, 16*(11), 7195-7211. https://doi.org/10.5194/acp-16-7195-2016

Hiranuma, N., Adachi, K., Bell, D. M., Belosi, F., Beydoun, H., Bhaduri, B., et al. (2019). A comprehensive characterization of ice nucleation by three different types of cellulose particles immersed in water. *Atmospheric Chemistry & Physics, 19*(7), 4823-4849. https://doi.org/10.5194/acp-19-4823-2019

Hiranuma, N., Möhler, O., Bingemer, H., Bundke, U., Cziczo, D. J., Danielczok, A., et al. (2013). Immersion freezing of clay minerals and bacterial ice nuclei. *AIP Conference Proceedings, 1527*(1), 914-917. https://doi.org/10.1063/1.4803420

Hiranuma, N., Möhler, O., Yamashita, K., Tajiri, T., Saito, A., Kiselev, A., et al. (2015). Ice nucleation by cellulose and its potential contribution to ice formation in clouds. *Nature Geoscience, 8*(4), 273-277. https://doi.org/10.1038/ngeo2374

Hoose, C., & Möhler, O. (2012). Heterogeneous ice nucleation on atmospheric aerosols: A review of results from laboratory experiments. *Atmospheric Chemistry & Physics, 12*(20), 9817-9854. https://doi.org/10.5194/acp-12-9817-2012

Hu, W., Murata, K., Toyonaga, S., & Zhang, D. (2017). Bacterial abundance and viability in rainwater associated with cyclones, stationary fronts and typhoons in southwestern Japan. *Atmospheric Environment, 167*, 104-115. https://doi.org/10.1016/j.atmosenv.2017.08.013

Huang, Q., Niu, S., Lü, J., Zhou, Y., & Zhang, X. (2018). Physical characteristics of freezing raindrop size distribution and terminal velocity in two ice weather cases in Lushan area. *Chinese Journal of Atmospheric Sciences, 42*(5), 1023-1037. http://d.old.wanfangdata.com.cn/Periodical/daqikx201805006

Huang, S., Hu, W., Chen, J., Wu, Z., Zhang, D., & Fu, P. (2021). Overview of biological ice nucleating particles in the atmosphere. *Environment International, 146*, 106197. https://doi.org/10.1016/j.envint.2020.106197

Huffman, J. A., Prenni, A. J., DeMott, P. J., Pöhlker, C., Mason, R. H., Robinson, N. H., et al. (2013). High concentrations of biological aerosol particles and ice nuclei during and after rain. *Atmospheric Chemistry & Physics, 13*(13), 6151-6164. https://doi.org/10.5194/acp-13-6151-2013

Iannone, R., Chernoff, D. I., Pringle, A., Martin, S. T., & Bertram, A. K. (2011). The ice nucleation ability of one of the most abundant types of fungal spores found in the atmosphere. *Atmospheric Chemistry & Physics, 11*(3), 1191-1201. https://doi.org/10.5194/acp-11-1191-2011

Joly, M., Amato, P., Deguillaume, L., Monier, M., Hoose, C., & Delort, A. M. (2014). Quantification of ice nuclei active at near 0 °C temperatures in low-altitude clouds at the Puy de Dôme atmospheric station. *Atmospheric Chemistry & Physics, 14*(15), 8185-8195. https://doi.org/10.5194/acp-14-8185-2014

Joyce, R. E., Lavender, H., Farrar, J., Werth, J. T., Weber, C. F., D'Andrilli, J., et al. (2019). Biological Ice-Nucleating Particles Deposited Year-Round in Subtropical Precipitation. *Applied and Environmental Microbiology, 85*(23), e01567-01519. https://doi.org/10.1128/aem.01567-19

Kanji, Z. A., Ladino, L. A., Wex, H., Boose, Y., Burkert-Kohn, M., Cziczo, D. J., & Krämer, M. (2017). Overview of ice nucleating particles. *Meteorological Monographs, 58*, 1.1–1.33. https://doi.org/10.1175/AMSMONOGRAPHS-D-16-0006.1

Karimi, B., Nosrati, R., Fazly, B., Mirpour, M., Malboobi, M. A., & Owlia, P. (2019). A comparative evaluation of freezing criteria and molecular characterization of epiphytic ice-nucleating (Ice +) and non-ice-nucleating (Ice −) *Pseudomonas syringae* and *Pseudomonas fluorescens*. *Journal of Plant Pathology, 102*, 1-10. https://doi.org/10.1007/s42161-019-00402-7

Kieft, T. L., & Ruscetti, T. (1990). Characterization of biological ice nuclei from a lichen. *Journal of Bacteriology, 172*(6), 3519-3523. https://doi.org/10.1128/jb.172.6.3519-3523.1990

Kilchhofer, K., Mahrt, F., & Kanji, Z. A. (2021). The role of cloud processing for the ice nucleating ability of organic aerosol and coal fly ash particles. *Journal of Geophysical Research: Atmospheres, 126*(10), e2020JD033338. https://doi.org/10.1029/2020JD033338

Kim, H. K., Orser, C., Lindow, S. E., & Sands, D. C. (1987). *Xanthomonas campestris* pv. *translucens* strains active in ice nucleation. *Plant Disease, 71*(11), 994-997. https://doi.org/10.1094/pd-71-0994

Kim, S., Kaplan, L. A., Benner, R., & Hatcher, P. G. (2004). Hydrogen-deficient molecules in natural riverine water samples—Evidence for the existence of black carbon in DOM. *Marine Chemistry, 92*(1), 225-234. https://doi.org/10.1016/j.marchem.2004.06.042

Klemm, O., & Wrzesinsky, T. (2007). Fog deposition fluxes of water and ions to a mountainous site in Central Europe. *Tellus B: Chemical and Physical Meteorology, 59*(4), 705-714. https://doi.org/10.1111/j.1600-0889.2007.00287.x

Klumpp, K., Marcolli, C., & Peter, T. (2022). The impact of (bio-)organic substances on the ice nucleation activity of the K-feldspar microcline in aqueous solutions. *Atmospheric Chemistry & Physics, 22*(5), 3655-3673. https://doi.org/10.5194/acp-22-3655-2022

Knopf, D. A., Alpert, P. A., & Wang, B. (2018). The role of organic aerosol in atmospheric ice nucleation: A review. *ACS Earth and Space Chemistry, 2*(3), 168-202. https://doi.org/10.1021/acsearthspacechem.7b00120

Kobashigawa, Y., Nishimiya, Y., Miura, K., Ohgiya, S., Miura, A., & Tsuda, S. (2005). A part of ice nucleation protein exhibits the ice-binding ability. *FEBS Letters, 579*(6), 1493-1497. https://doi.org/10.1016/j.febslet.2005.01.056

Koch, B. P., Dittmar, T., Witt, M., & Kattner, G. (2007). Fundamentals of molecular formula assignment to ultrahigh resolution mass data of natural organic matter. *Analytical Chemistry, 79*(4), 1758-1763. https://doi.org/10.1021/ac061949s

Koop, T., & Zobrist, B. (2009). Parameterizations for ice nucleation in biological and atmospheric systems. *Physical Chemistry Chemical Physics, 11*(46), 10839-10850. https://doi.org/10.1039/B914289D

Krog, J. O., Zachariassen, K. E., Larsen, B., & Smidsrød, O. (1979). Thermal buffering in Afro-alpine plants due to nucleating agent-induced water freezing. *Nature, 282*, 300-301. https://doi.org/10.1038/282300a0

Kunert, A. T., Pöhlker, M. L., Tang, K., Krevert, C. S., Wieder, C., Speth, K. R., et al. (2019). Macromolecular fungal ice nuclei in *Fusarium*: Effects of physical and chemical processing. *Biogeosciences, 16*(23), 4647-4659. https://doi.org/10.5194/bg-16-4647-2019

Lacher, L., Steinbacher, M., Bukowiecki, N., Herrmann, E., Zipori, A., & Kanji, Z. A. (2018). Impact of Air Mass Conditions and Aerosol Properties on Ice Nucleating Particle Concentrations at the High Altitude Research Station Jungfraujoch. *Atmosphere, 9*(9), 363. https://doi.org/10.3390/atmos9090363

Li, P., Wang, Y., Li, T., Sun, L., Yi, X., Guo, L., & Su, R. (2015). Characterization of carbonaceous aerosols at Mount Lu in South China: implication for secondary organic carbon formation and long-range transport. *Environmental Science and Pollution Research, 22*(18), 14189-14199. https://doi.org/10.1007/s11356-015-4654-9

Lim, Y. B., Tan, Y., Perri, M. J., Seitzinger, S. P., & Turpin, B. J. (2010). Aqueous chemistry and its role in secondary organic aerosol (SOA) formation. *Atmospheric Chemistry & Physics, 10*(21), 10521-10539. https://doi.org/10.5194/acp-10-10521-2010

Lindow, S., Lahue, E., Govindarajan, A., Panopoulos, N., & Gies, D. (1989). Localization of ice nucleation activity and the iceC gene product in *Pseudomonas syringae* and *Escherichia coli*. *Molecular Plant-Microbe Interact, 2*(5), 262-272. https://doi.org/10.1094/MPMI-2-262

Lohmann, U., & Feichter, J. (2005). Global indirect aerosol effects: A review. *Atmospheric Chemistry & Physics, 5*(3), 715-737. https://doi.org/10.5194/acp-5-715-2005

Maki, L. R., Galyan, E. L., Chang-Chien, M.-M., & Caldwell, D. R. (1974). Ice nucleation induced by *Pseudomonas syringae*. *Applied Microbiology, 28*(3), 456-459. https://doi.org/10.1128/am.28.3.456-459.1974

Martin, A. C., Cornwell, G., Beall, C. M., Cannon, F., Reilly, S., Schaap, B., et al. (2019). Contrasting local and long-range-transported warm ice-nucleating particles during an atmospheric river in coastal California, USA. *Atmospheric Chemistry & Physics, 19*(7), 4193-4210. https://doi.org/10.5194/acp-19-4193-2019

Masschalck, B., & Michiels, C. W. (2003). Antimicrobial properties of lysozyme in relation to foodborne vegetative bacteria. *Critical Reviews in Microbiology, 29*(3), 191-214. https://doi.org/10.1080/713610448

Michaud, A. B., Dore, J. E., Leslie, D., Lyons, W. B., Sands, D. C., & Priscu, J. C. (2014). Biological ice nucleation initiates hailstone formation. *Journal of Geophysical Research: Atmospheres, 119*(21), 12186-12197. https://doi.org/10.1002/2014JD022004

Miller, A. J., Brennan, K. P., Mignani, C., Wieder, J., David, R. O., & Borduas-Dedekind, N. (2021). Development of the drop Freezing Ice Nuclei Counter (FINC), intercomparison of droplet freezing techniques, and use of soluble lignin as an atmospheric ice nucleation standard. *Atmospheric Measurement Techniques, 14*(4), 3131-3151. https://doi.org/10.5194/amt-14-3131-2021

Möhler, O., Benz, S., Saathoff, H., Schnaiter, M., Wagner, R., Schneider, J., et al. (2008). The effect of organic coating on the heterogeneous ice nucleation efficiency of mineral dust aerosols. *Environmental Research Letters, 3*(2), 025007. https://doi.org/10.1088/1748-9326/3/2/025007

Morris, C. E., Georgakopoulos, D. G., & Sands, D. C. (2004). *Ice nucleation active bacteria and their potential role in precipitation*. Paper presented at the Journal de Physique IV France.

Morris, C. E., Sands, D. C., Glaux, C., Samsatly, J., Asaad, S., Moukahel, A. R., et al. (2013). Urediospores of rust fungi are ice nucleation active at > −10 °C and harbor ice nucleation active bacteria. *Atmospheric Chemistry & Physics, 13*(8), 4223-4233. https://doi.org/10.5194/acp-13-4223-2013

Mortazavi, R., Hayes, C. T., & Ariya, P. A. (2008). Ice nucleation activity of bacteria isolated from snow compared with organic and inorganic substrates. *Environmental Chemistry, 5*(6), 373-381. https://doi.org/10.1071/EN08055

Murray, E., Murray, B., & Sivakumar, V. (2013). Ice nucleation by particles immersed in supercooled cloud droplets. *Chemical Society Reviews, 42*, 9571-9572. https://doi.org/10.1039/C2CS35200A

Niu, M., Hu, W., & Fu, P. (2024). Deciphering the significant role of biological ice nucleators in precipitation at the organic molecular level [Dataset]. *Zenodo*. https://doi.org/10.5281/zenodo.10300240

O'Sullivan, D., Murray, B. J., Malkin, T. L., Whale, T. F., Umo, N. S., Atkinson, J. D., et al. (2014). Ice nucleation by fertile soil dusts: Relative importance of mineral and biogenic components. *Atmospheric Chemistry & Physics, 14*(4), 1853-1867. https://doi.org/10.5194/acp-14-1853-2014

O'Sullivan, D., Murray, B. J., Ross, J. F., & Webb, M. E. (2016). The adsorption of fungal ice-nucleating proteins on mineral dusts: A terrestrial reservoir of atmospheric ice-nucleating particles. *Atmospheric Chemistry & Physics, 16*(12), 7879-7887. https://doi.org/10.5194/acp-16-7879-2016

O′ Sullivan, D., Murray, B. J., Ross, J. F., Whale, T. F., Price, H. C., Atkinson, J. D., et al. (2015). The relevance of nanoscale biological fragments for ice nucleation in clouds. *Scientific Reports, 5*(1), 8082. https://doi.org/10.1038/srep08082

Obata, H., Nakai, T., Tanishita, J., & Tokuyama, T. (1989). Identification of an ice–nucleating bacterium and its ice nucleation properties. *Journal of Fermentation and Bioengineering, 67*, 143–147. https://doi.org/10.1016/0922-338X（89）90111-6

Obata, H., Saeki, Y., Tanishita, J., Tokuyama, T., Hori, H., & Higashi, Y. (1987). Studies on ice-nucleating microorganisms. Part I. Identification of an ice-nucleating bacterium KUIN-1 as *Pseudomonas* fluorescens and its ice nucleation properties. *Agricultural and Biological Chemistry, 51*, 1761–1766. https://doi.org/10.1016/0922-338X（89）90111-6

Pereira, D. L., Silva, M. M., García, R., Raga, G. B., Alvarez-Ospina, H., Carabali, G., et al. (2021). Characterization of ice nucleating particles in rainwater, cloud water, and aerosol samples at two different tropical latitudes. *Atmospheric Research, 250*, 105356. https://doi.org/10.1016/j.atmosres.2020.105356

Petters, M. D., & Wright, T. P. (2015). Revisiting ice nucleation from precipitation samples. *Geophysical Research Letters, 42*(20), 8758-8766. https://doi.org/10.1002/2015GL065733

Pouleur, S., Richard, C., Martin, J. G., & Antoun, H. (1992). Ice Nucleation Activity in *Fusarium acuminatum* and *Fusarium avenaceum*. *Applied and Environmental Microbiology, 58*(9), 2960-2964. https://doi.org/10.1128/aem.58.9.2960-2964.1992

Pouzet, G., Peghaire, E., Aguès, M., Baray, J.-L., Conen, F., & Amato, P. (2017). Atmospheric processing and variability of biological ice nucleating particles in precipitation at Opme, France. *Atmosphere, 8*(11), 229. https://doi.org/10.3390/atmos8110229

Pruppacher, H. R., & Klett, J. D. (2010). *Microphysics of clouds and precipitation* (Vol. 18): Springer Dordrecht.

Pummer, B. G., Bauer, H., Bernardi, J., Bleicher, S., & Grothe, H. (2012). Suspendable macromolecules are responsible for ice nucleation activity of birch and conifer pollen. *Atmospheric Chemistry & Physics, 12*(5), 2541-2550. https://doi.org/10.5194/acp-12-2541-2012

Pummer, B. G., Budke, C., Augustin-Bauditz, S., Niedermeier, D., Felgitsch, L., Kampf, C. J., et al. (2015). Ice nucleation by water-soluble macromolecules. *Atmospheric Chemistry & Physics, 15*(8), 4077-4091. https://doi.org/10.5194/acp-15-4077-2015

R-Core-Team. (2012). R: A Language and Environment for Statistical Computing [Software]. *R Foundation for Statistical Computing*. http://www.r-project.org/

Rederstorff, E., Fatimi, A., Sinquin, C., Ratiskol, J., Merceron, C., Vinatier, C., et al. (2011). Sterilization of exopolysaccharides produced by deep-sea bacteria: Impact on their stability and degradation. *Marine Drugs, 9*(2), 224-241. https://doi.org/10.3390/md9020224

Repaske, R. (1956). Lysis of gram-negative bacteria by lysozyme. *Biochimica et Biophysica Acta, 22*(1), 189-191. https://doi.org/10.1016/0006-3002(56)90240-2

Rice, C. V., Middaugh, A., Wickham, J. R., Friedline, A., Thomas, K. J., Scull, E., et al. (2015). Bacterial lipoteichoic acid enhances cryosurvival. *Extremophiles, 19*(2), 297-305. https://doi.org/10.1007/s00792-014-0714-1

Rodríguez Zafra, J. M., de Cara García, M., Tello Marquina, J., & Palmero Llamas, D. (2016). Dispersal of *Fusarium* spp. by rainwater and pathogenicity on four plant species. *Aerobiologia, 32*(3), 431-439. https://doi.org/10.1007/s10453-015-9416-0

Šantl-Temkiv, T., Lange, R., Beddows, D., Rauter, U., Pilgaard, S., Dall'Osto, M., et al. (2019). Biogenic sources of ice nucleating particles at the High Arctic site villum research station. *Environmental Science & Technology, 53*(18), 10580-10590. https://doi.org/10.1021/acs.est.9b00991

Šantl-Temkiv, T., Sahyoun, M., Finster, K., Hartmann, S., Augustin-Bauditz, S., Stratmann, F., et al. (2015). Characterization of airborne ice-nucleation-active bacteria and bacterial fragments. *Atmospheric Environment, 109*, 105-117. https://doi.org/10.1016/j.atmosenv.2015.02.060

Schmieder, R., & Edwards, R. (2011). Quality control and preprocessing of metagenomic datasets. *Bioinformatics, 27*(6), 863-864. https://doi.org/10.1093/bioinformatics/btr026

Schnell, R. C. (1977). Ice nuclei in seawater, fog water and marine air off the coast of Nova Scotia: Summer 1975. *Journal of Atmospheric Sciences, 34*(8), 1299-1305. https://doi.org/10.1175/1520-0469(1977)034<1299:INISFW>2.0.CO;2

Schnell, R. C., & Vali, G. (1973). World-wide source of leaf-derived freezing nuclei. *Nature, 246*(5430), 212-213. https://doi.org/10.1038/246212a0

Schnell, R. C., & Vali, G. (1976). Biogenic ice nuclei: Part I. Terrestrial and marine sources. *Journal of Atmospheric Sciences, 33*(8), 1554-1564. https://doi.org/10.1175/1520-0469(1976)033<1554:Binpit>2.0.Co;2

Steiner, A. L., Brooks, S. D., Deng, C., Thornton, D. C. O., Pendleton, M. W., & Bryant, V. (2015). Pollen as atmospheric cloud condensation nuclei. *Geophysical Research Letters, 42*(9), 3596-3602. https://doi.org/10.1002/2015GL064060

Steinke, I., Hiranuma, N., Funk, R., Höhler, K., Tüllmann, N., Umo, N. S., et al. (2020). Complex plant-derived organic aerosol as ice-nucleating particles – more than the sums of their parts? *Atmospheric Chemistry & Physics, 20*(19), 11387-11397. https://doi.org/10.5194/acp-20-11387-2020

Stopelli, E., Conen, F., Guilbaud, C., Zopfi, J., Alewell, C., & Morris, C. E. (2017). Ice nucleators, bacterial cells and *Pseudomonas syringae* in precipitation at Jungfraujoch. *Biogeosciences, 14*(5), 1189-1196. https://doi.org/10.5194/bg-14-1189-2017

Stopelli, E., Conen, F., Morris, C. E., Herrmann, E., Henne, S., Steinbacher, M., & Alewell, C. (2016). Predicting abundance and variability of ice nucleating particles in precipitation at the high-altitude observatory Jungfraujoch. *Atmospheric Chemistry & Physics, 16*(13), 8341-8351. https://doi.org/10.5194/acp-16-8341-2016

Sun, X., Wang, Y., Li, H., Yang, X., Sun, L., Wang, X., et al. (2016). Organic acids in cloud water and rainwater at a mountain site in acid rain areas of South China. *Environmental Science and Pollution Research, 23*(10), 9529-9539. https://doi.org/10.1007/s11356-016-6038-1

Sze, K. C. H., Wex, H., Hartmann, M., Skov, H., Massling, A., Villanueva, D., & Stratmann, F. (2023). Ice-nucleating particles in northern Greenland: Annual cycles, biological contribution and parameterizations. *Atmospheric Chemistry & Physics, 23*(8), 4741-4761. https://doi.org/10.5194/acp-23-4741-2023

Tang, K., Sanchez-Parra, B., Yordanova, P., Wehking, J., Backes, A. T., Pickersgill, D. A., et al. (2022). Bioaerosols and atmospheric ice nuclei in a Mediterranean dryland: Community changes related to rainfall. *Biogeosciences, 19*(1), 71-91. https://doi.org/10.5194/bg-19-71-2022

Testa, B., Hill, T. C. J., Marsden, N. A., Barry, K. R., Hume, C. C., Bian, Q., et al. (2021). Ice nucleating particle connections to regional argentinian land surface emissions and weather during the cloud, aerosol, and complex terrain interactions experiment. *Journal of Geophysical Research: Atmospheres, 126*(23), e2021JD035186. https://doi.org/10.1029/2021JD035186

Tobo, Y., Adachi, K., DeMott, P. J., Hill, T. C. J., Hamilton, D. S., Mahowald, N. M., et al. (2019). Glacially sourced dust as a potentially significant source of ice nucleating particles. *Nature Geoscience, 12*(4), 253-258. https://doi.org/10.1038/s41561-019-0314-x

Tobo, Y., DeMott, P. J., Hill, T. C. J., Prenni, A. J., Swoboda-Colberg, N. G., Franc, G. D., & Kreidenweis, S. M. (2014). Organic matter matters for ice nuclei of agricultural soil origin. *Atmospheric Chemistry & Physics, 14*(16), 8521-8531. https://doi.org/10.5194/acp-14-8521-2014

Urano, M., & Douple, E. B. (2023). *Thermal Effects on Cells and Tissues* (Vol. 1). London: CRC Press.

Vali, G. (1971). Quantitative evaluation of experimental results an the heterogeneous freezing nucleation of supercooled liquids. *Journal of Atmospheric Sciences, 28*(3), 402-409. https://doi.org/10.1175/1520-0469(1971)028<0402:QEOERA>2.0.CO;2

Vali, G., DeMott, P. J., Möhler, O., & Whale, T. F. (2015). Technical Note: A proposal for ice nucleation terminology. *Atmospheric Chemistry & Physics, 15*(18), 10263-10270. https://doi.org/10.5194/acp-15-10263-2015

Walters, K. R., Serianni, A. S., Sformo, T., Barnes, B. M., & Duman, J. G. (2009). A nonprotein thermal hysteresis-producing xylomannan antifreeze in the freeze-tolerant Alaskan beetle *Upis ceramboides*. *Proceedings of the National Academy of Sciences, 106*(48), 20210-20215. https://doi.org/10.1073/pnas.0909872106

Wang, B., & Knopf, D. A. (2011). Heterogeneous ice nucleation on particles composed of humic-like substances impacted by O_3. *Journal of Geophysical Research: Atmospheres, 116*(D3), D03205. https://doi.org/10.1029/2010JD014964

Watabe, S., Abe, K., Hirata, A., Emori, Y., Watanabe, M., & Arai, S. (1993). Large-scale Production and Purification of an Erwinia ananas Ice Nucleation Protein and Evaluation of Its Ice Nucleation Activity. *Bioscience, Biotechnology, and Biochemistry, 57*(4), 603-606. https://doi.org/10.1271/bbb.57.603

Wilson, T. W., Ladino, L. A., Alpert, P. A., Breckels, M. N., Brooks, I. M., Browse, J., et al. (2015). A marine biogenic source of atmospheric ice-nucleating particles. *Nature, 525*(7568), 234-238. https://doi.org/10.1038/nature14986

Wise, M. E., Baustian, K. J., Koop, T., Freedman, M. A., Jensen, E. J., & Tolbert, M. A. (2012). Depositional ice nucleation onto crystalline hydrated NaCl particles: A new mechanism for ice formation in the troposphere. *Atmospheric Chemistry & Physics, 12*(2), 1121-1134. https://doi.org/10.5194/acp-12-1121-2012

Wolber, P., & Warren, G. (1989). Bacterial ice-nucleation proteins. *Trends in Biochemical Sciences, 14*(5), 179-182. https://doi.org/10.1016/0968-0004(89)90270-3

Xu, H., Griffith, M., Patten, C. L., & Glick, B. R. (1998). Isolation and characterization of an antifreeze protein with ice nucleation activity from the plant growth promoting rhizobacterium *Pseudomonas putida* GR12-2. *Canadian Journal of Microbiology, 44*(1), 64-73. https://doi.org/10.1139/w97-126

Yamashita, Y., Kawahara, H., & Obata, H. (2002). Identification of a novel anti-ice-nucleating polysaccharide from *Bacillus thuringiensis* YY529. *Bioscience, Biotechnology, and Biochemistry, 66*(5), 948-954. https://doi.org/10.1271/bbb.66.948

Yang, L., Chen, W., Zhuang, W.-E., Cheng, Q., Li, W., Wang, H., et al. (2019). Characterization and bioavailability of rainwater dissolved organic matter at the southeast coast of China using absorption spectroscopy and fluorescence EEM-PARAFAC. *Estuarine, Coastal and Shelf Science, 217*, 45-55. https://doi.org/10.1016/j.ecss.2018.11.002

Yanti, Y., Zainon, M. N., & Marshida, A. H. U. (2012, 23-26 Sept. 2012). *Antagonistic activity of three Actinomycetes, MG01, MG02 And KT2F towards Phellinus noxius.* Paper presented at the 2012 IEEE Symposium on Business, Engineering and Industrial Applications.

Zhang, S., Du, R., Chen, H., Zhang, Y., Du, P., & Ren, W. (2020). Characteristics and Distribution of efficient ice nucleating particles in rainwater and soil. *Atmospheric Research, 246*, 105129. https://doi.org/10.1016/j.atmosres.2020.105129

Zhou, L., Zhou, Y., Hu, Y., Cai, J., Liu, X., Bai, C., et al. (2019). Microbial production and consumption of dissolved organic matter in glacial ecosystems on the Tibetan Plateau. *Water Research, 160*, 18-28. https://doi.org/10.1016/j.watres.2019.05.048

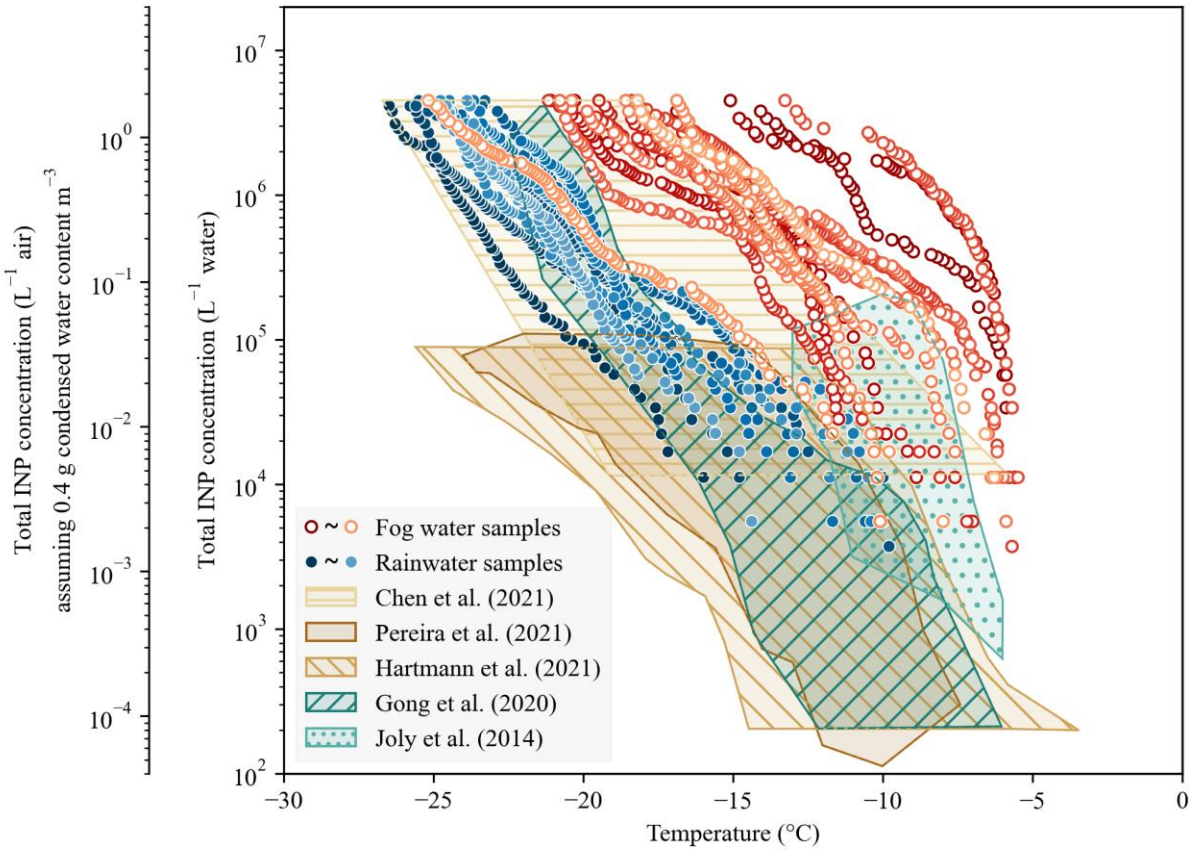

Figure 1. Total concentrations of ice nucleating particles in precipitation samples. The cumulative ice nucleating particle (INP) spectra per unit volume of rainwater samples (blue dots) and fog water samples (red dots) were performed by droplet freezing assays. The INP spectra per volume of air were calculated by assuming a cloud-condensed water content of 0.4 g m^{-3} according to Chen, Wu, Wu, et al. (2021). The shaded area represents the total INP concentrations in precipitation samples measured by other studies (Chen, Wu, Wu, et al., 2021; Gong et al., 2020; Hartmann et al., 2021; Joly et al., 2014; Pereira et al., 2021).

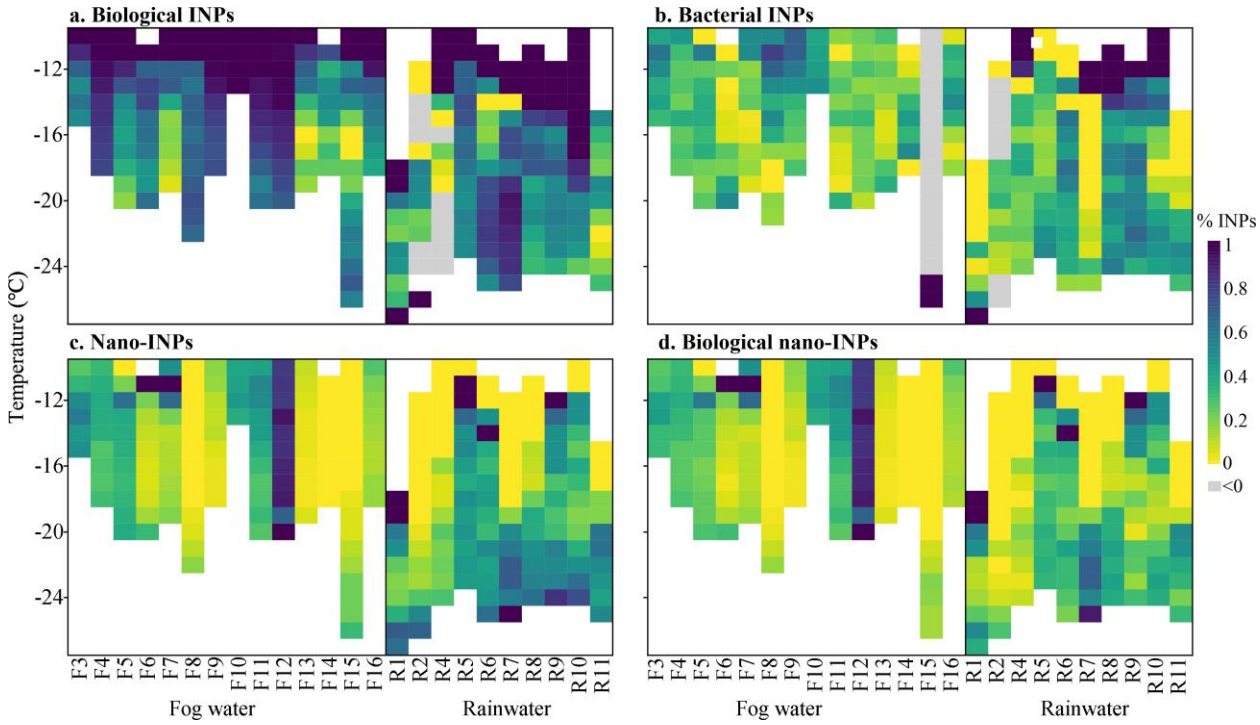

Figure 2. Contribution of biological materials to total ice nucleating particles. Variations in the percentages of heat-sensitive ice nucleating particles (INPs) (a, regarded as biological INPs in this study) and lysozyme-sensitive INPs (b, regarded as bacterial INPs) to total INPs were observed at different temperatures. (c) and (d) represent the proportions of nanoscale INPs (nano-INPs, INPs smaller than 0.22 μm herein) and heat-sensitive nano-INPs (biological nano-INPs) to total INPs, respectively.

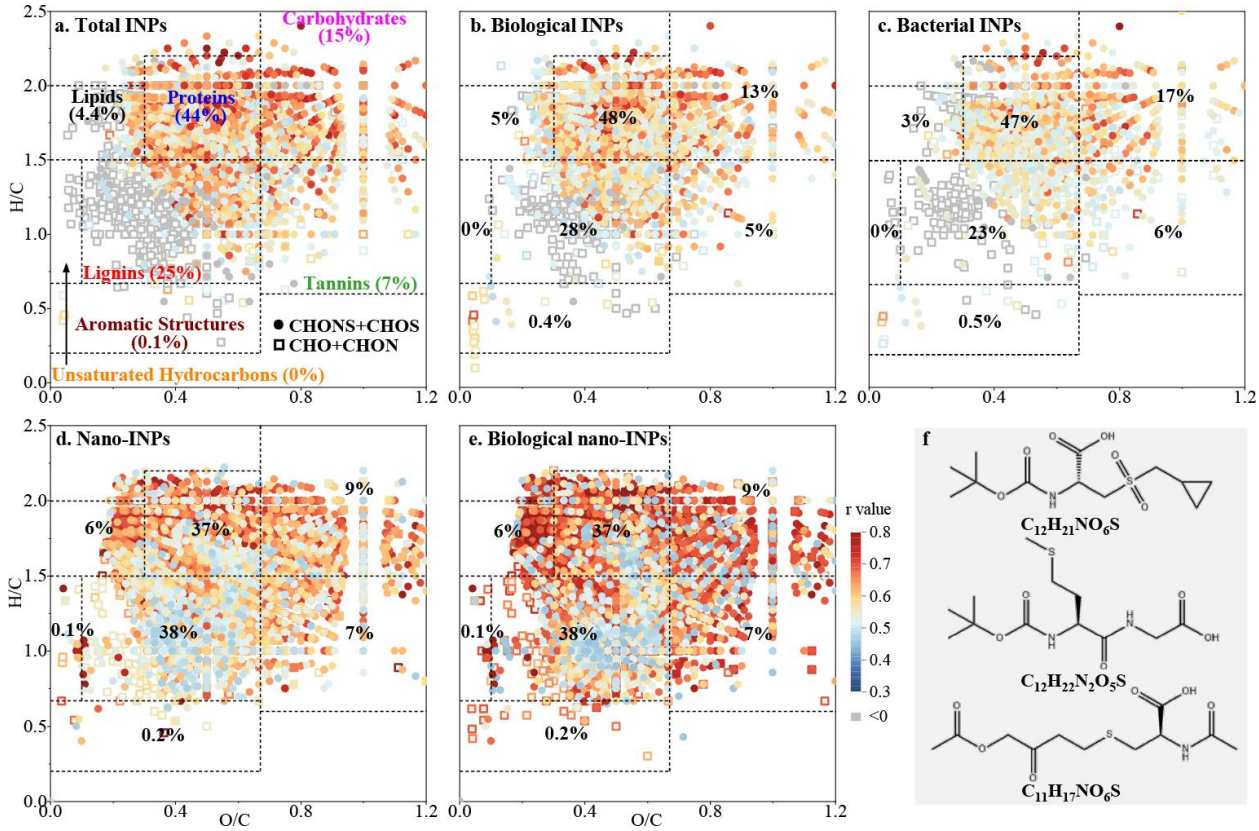

Figure 3. Organic molecular composition associated with different types of ice nucleating particles. The organic molecules significantly correlated with the concentrations of total (a), biological (b) and bacterial (c) ice nucleating particles (INPs) at −18°C, and nanoscale INPs (nano-INPs) (d) and biological nano-INPs (e) at −20°C based on Spearman correlation analysis ($p < 0.05$) and their classification are presented by van Krevelen diagrams. The fractional contributions to the organic molecules are shown for each molecular class. The contributions of sulfur-containing compounds (CHOS and CHONS, circle) and non-sulfur-containing compounds (CHO and CHON, square) to total organic molecules correlated with different types of INPs are shown. **f** shows the possible structures of sulfur-containing compounds associated with INPs based on molecular formulas.

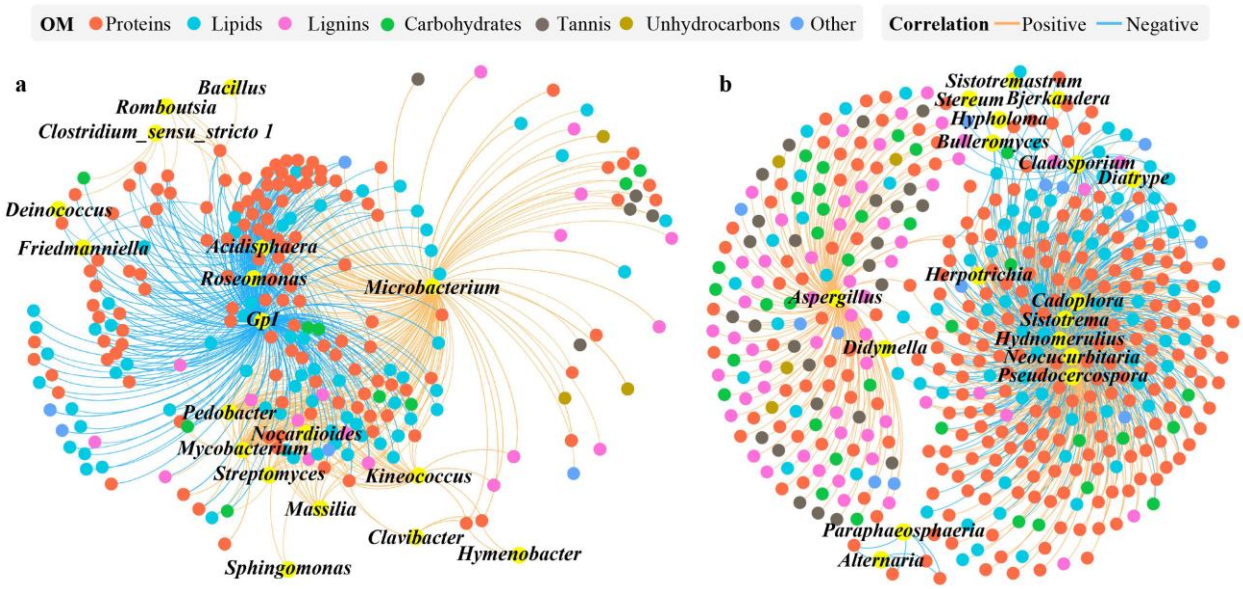

Figure 4. Association between microbial taxa and nanoscale ice nucleating particles-related organic matter. Co-occurrence networks of biological nanoscale ice nucleating particles-related organic matter (OM) were constructed based on Spearman's correlation analysis with bacterial (a) and fungal (b) genera, respectively. Only OM molecules significantly correlated with biological nanoscale ice nucleating particles (Spearman's correlation coefficient > 0.7) were applied for network construction. Microbial genera are labeled in yellow in networks.

Figure 1.

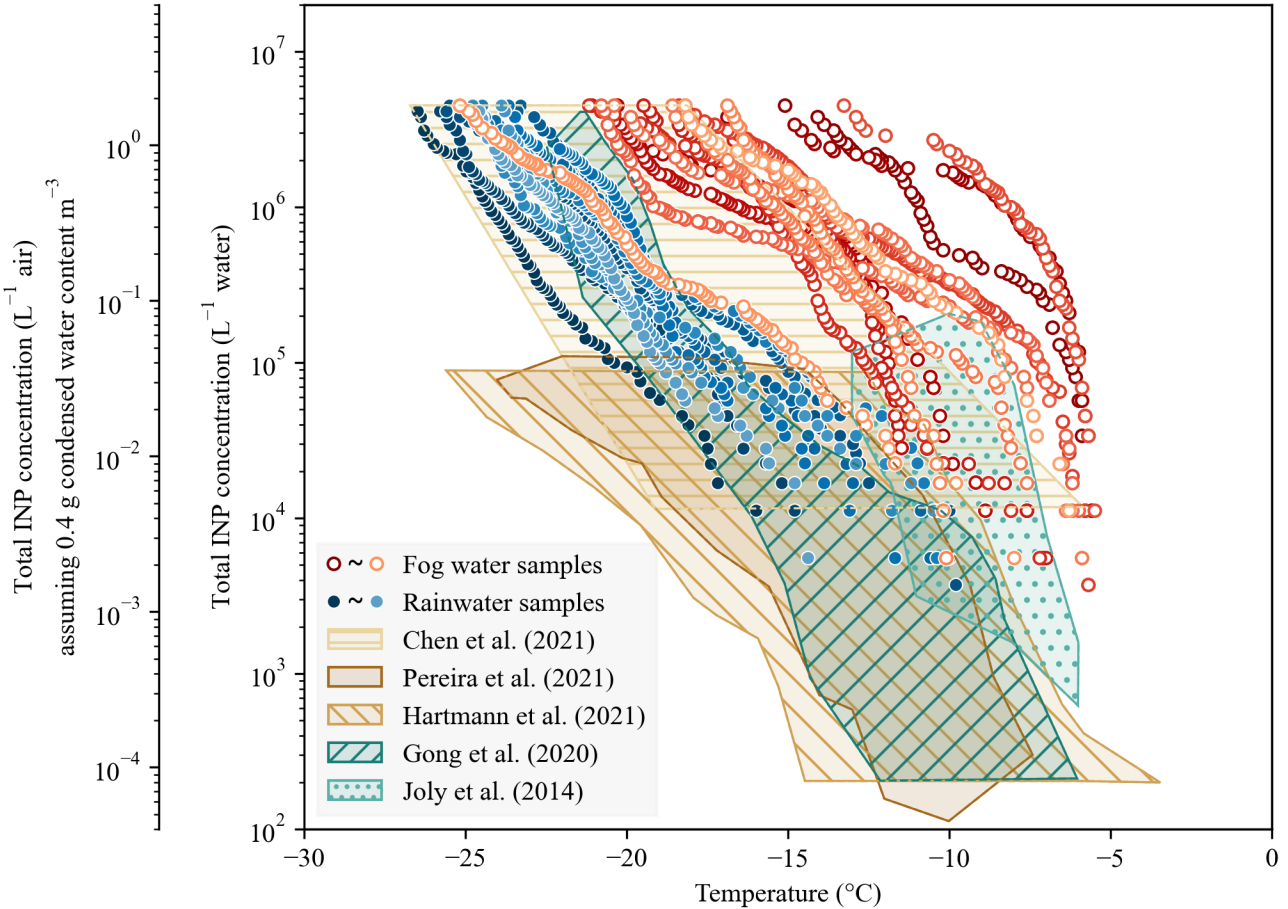
Total INP concentration (L^{-1} air)
assuming 0.4 g condensed water content m^{-3}
10^{0}
10^{-1}
10^{-2}
10^{-3}
10^{-4}
Total INP concentration (L^{-1} water)
10^{7}
10^{6}
10^{5}
10^{4}
10^{3}
10^{2}
−30
−25
−20
−15
−10
−5
0
Temperature (°C)
Fog water samples
Rainwater samples
Chen et al. (2021)
Pereira et al. (2021)
Hartmann et al. (2021)
Gong et al. (2020)
Joly et al. (2014)

Figure 2.

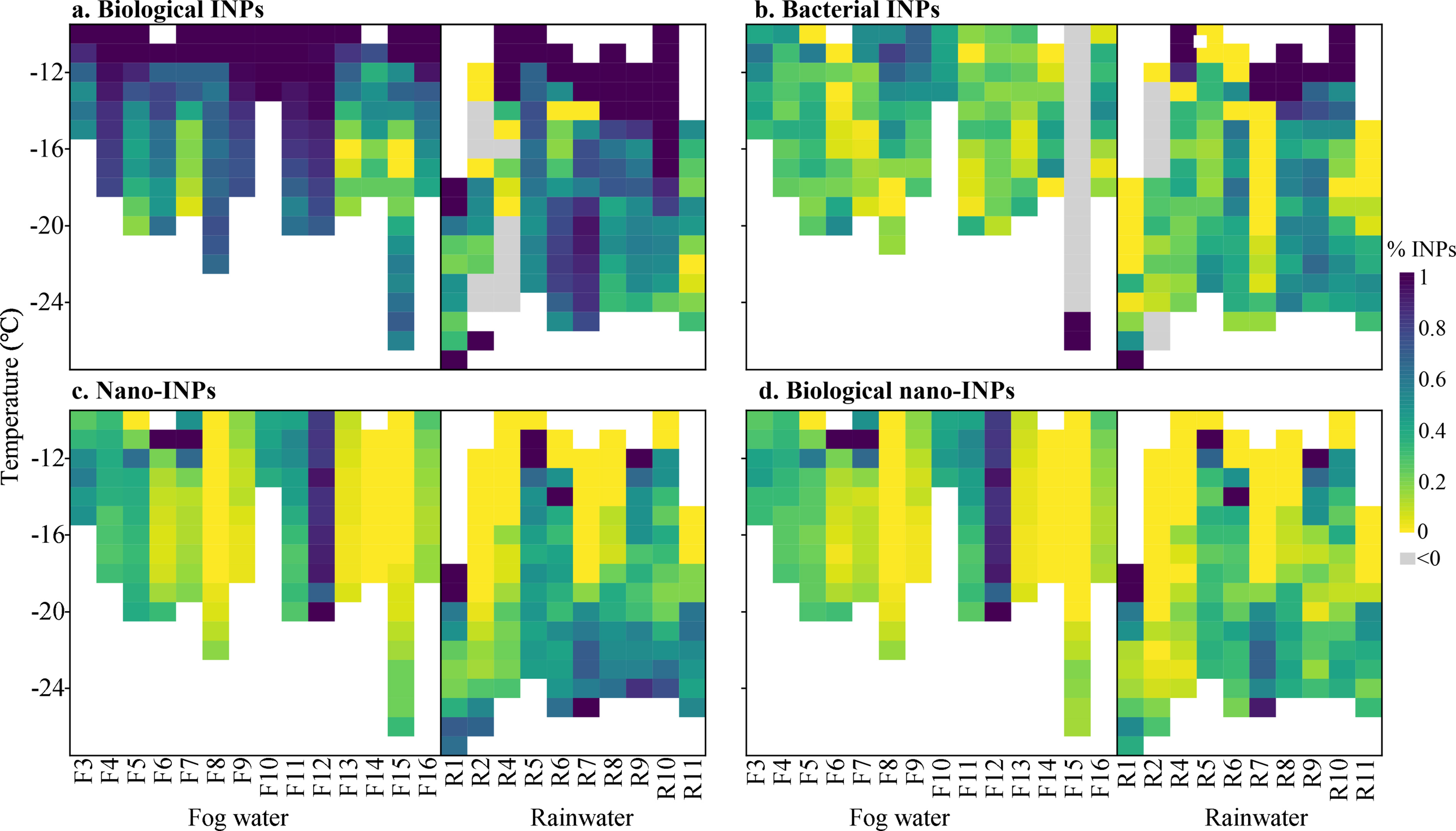
a. Biological INPs
b. Bacterial INPs
c. Nano-INPs
d. Biological nano-INPs
Temperature (ºC)
-12
-16
-20
-24
% INPs
1
0.8
0.6
0.4
0.2
0
<0
F3 F4 F5 F6 F7 F8 F9 F10 F11 F12 F13 F14 F15 F16 R1 R2 R4 R5 R6 R7 R8 R9 R10 R11
Fog water
Rainwater

Figure 3.

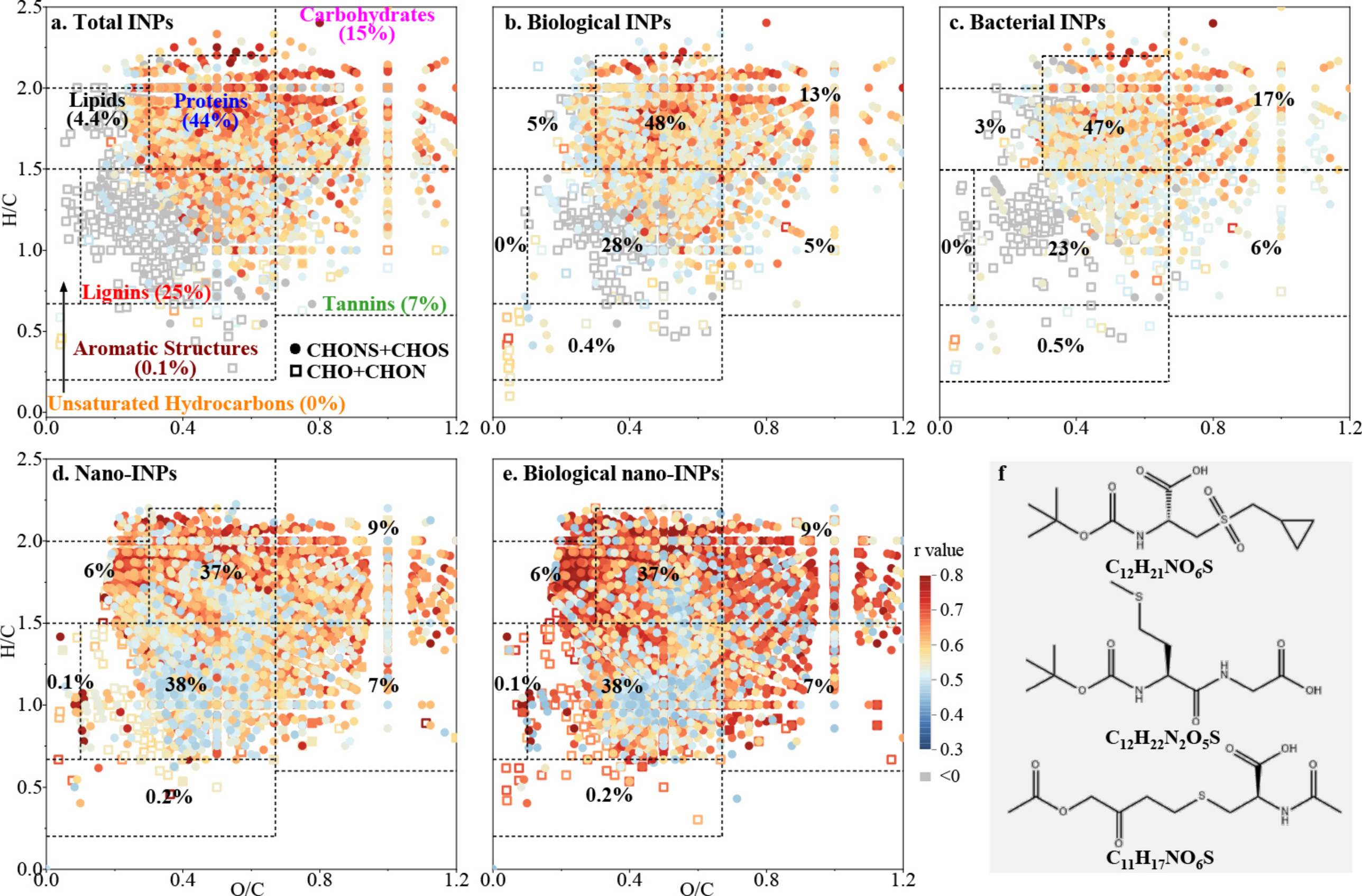
a. Total INPs
Carbohydrates (15%)
Lipids (4.4%)
Proteins (44%)
Lignins (25%)
Tannins (7%)
Aromatic Structures (0.1%)
Unsaturated Hydrocarbons (0%)
CHONS+CHOS
CHO+CHON
b. Biological INPs
13%
5%
48%
0%
28%
5%
0.4%
c. Bacterial INPs
17%
3%
47%
0%
23%
6%
0.5%
d. Nano-INPs
9%
6%
37%
0.1%
38%
7%
0.2%
e. Biological nano-INPs
9%
6%
37%
0.1%
38%
7%
0.2%
H/C
O/C
r value
0.8
0.7
0.6
0.5
0.4
0.3
<0
f
$C_{12}H_{21}NO_6S$
$C_{12}H_{22}N_2O_5S$
$C_{11}H_{17}NO_6S$

Figure 4.

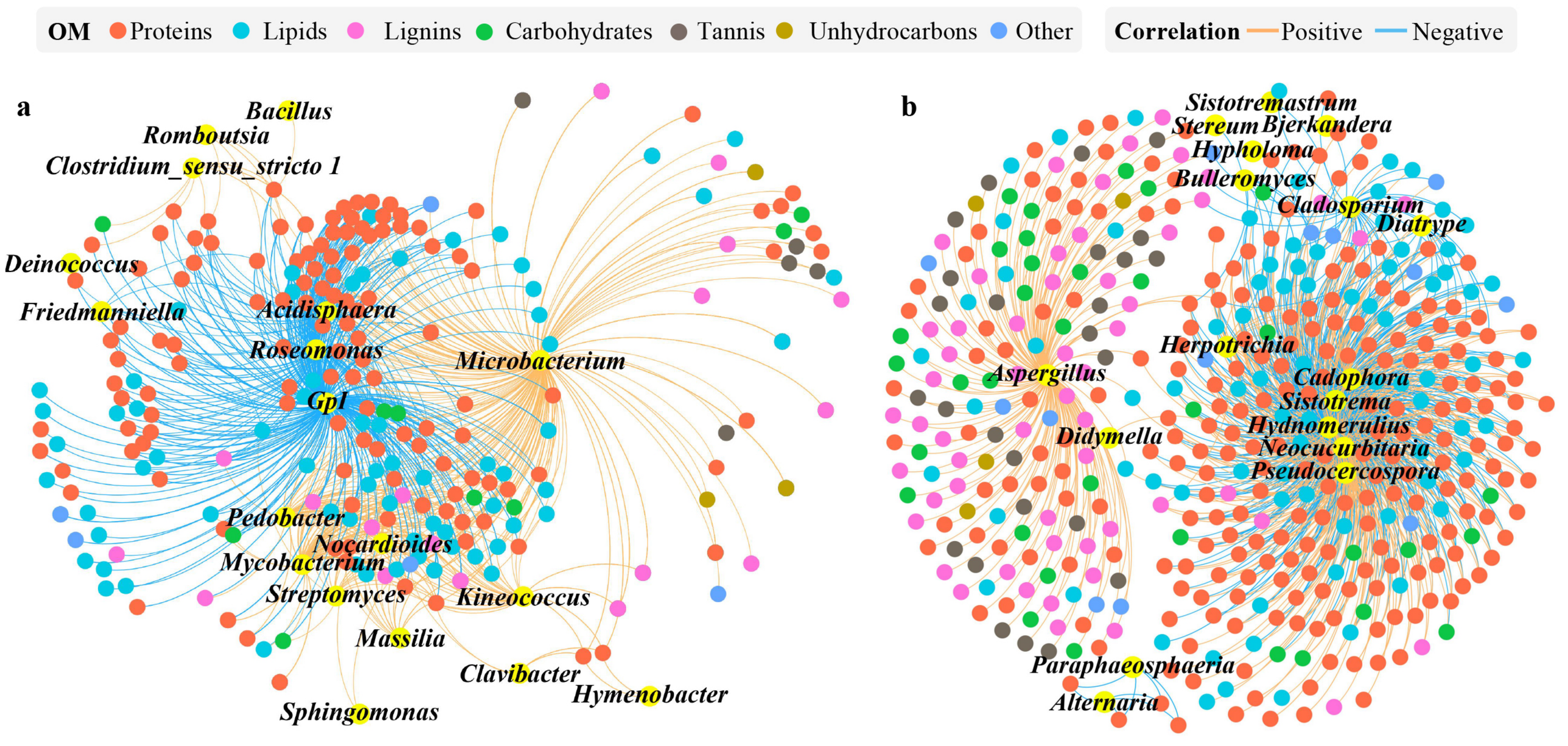
OM
Proteins
Lipids
Lignins
Carbohydrates
Tannis
Unhydrocarbons
Other
Correlation
Positive
Negative
a
Bacillus
Romboutsia
Clostridium_sensu_stricto 1
Deinococcus
Friedmanniella
Acidisphaera
Roseomonas
Microbacterium
Gp1
Pedobacter
Nocardioides
Mycobacterium
Streptomyces
Kineococcus
Massilia
Clavibacter
Hymenobacter
Sphingomonas
b
Sistotremastrum
Stereum
Bjerkandera
Hypholoma
Bulleromyces
Cladosporium
Diatrype
Herpotrichia
Aspergillus
Cadophora
Sistotrema
Hydnomerulius
Didymella
Neocucurbitaria
Pseudocercospora
Paraphaeosphaeria
Alternaria

Journal of Geophysical Research: Atmospheres

Supporting Information for

Deciphering the significant role of biological ice nucleators in precipitation at the organic molecular level

Mutong Niu[1], Wei Hu[1, *], Shu Huang[1], Jie Chen[2], Shujun Zhong[1], Ziye Huang[1], Peimin Duan[1], Xiangyu Pei[3], Jing Duan[4], Kai Bi[5], Shuang Chen[1], Rui Jin[1], Ming Sheng[1], Ning Yang[1], Libin Wu[1], Junjun Deng[1], Jialei Zhu[1], Fangxia Shen[6], Zhijun Wu[7], Daizhou Zhang[8], Pingqing Fu[1, *]

[1]Institute of Surface-Earth System Science, School of Earth System Science, Tianjin University, Tianjin 300072, China

[2]Institute for Atmospheric and Climate Science, ETH Zürich, Zurich 8092, Switzerland

[3]College of Environmental and Resource Sciences, Zhejiang Provincial Key Laboratory of Organic Pollution Process and Control, Zhejiang University, Hangzhou 310058, China

[4]State Key Laboratory of Severe Weather & Key Laboratory for Cloud Physics, Chinese Academy of Meteorological Sciences, Beijing 100081, China

[5]Beijing Key Laboratory of Cloud, Precipitation, and Atmospheric Water Resources, Beijing Weather Modification Office (BWMO), Beijing 100089, China

[6]School of Energy and Power Engineering, Beihang University, Beijing 102206, China

[7]State Key Joint Laboratory of Environmental Simulation and Pollution Control, College of Environmental Sciences and Engineering, Peking University, Beijing 100081, China

[8]Faculty of Environmental and Symbiotic Sciences, Prefectural University of Kumamoto, Kumamoto 862-8502, Japan

Contents of this file

Introduction

This supporting information includes figures and tables.

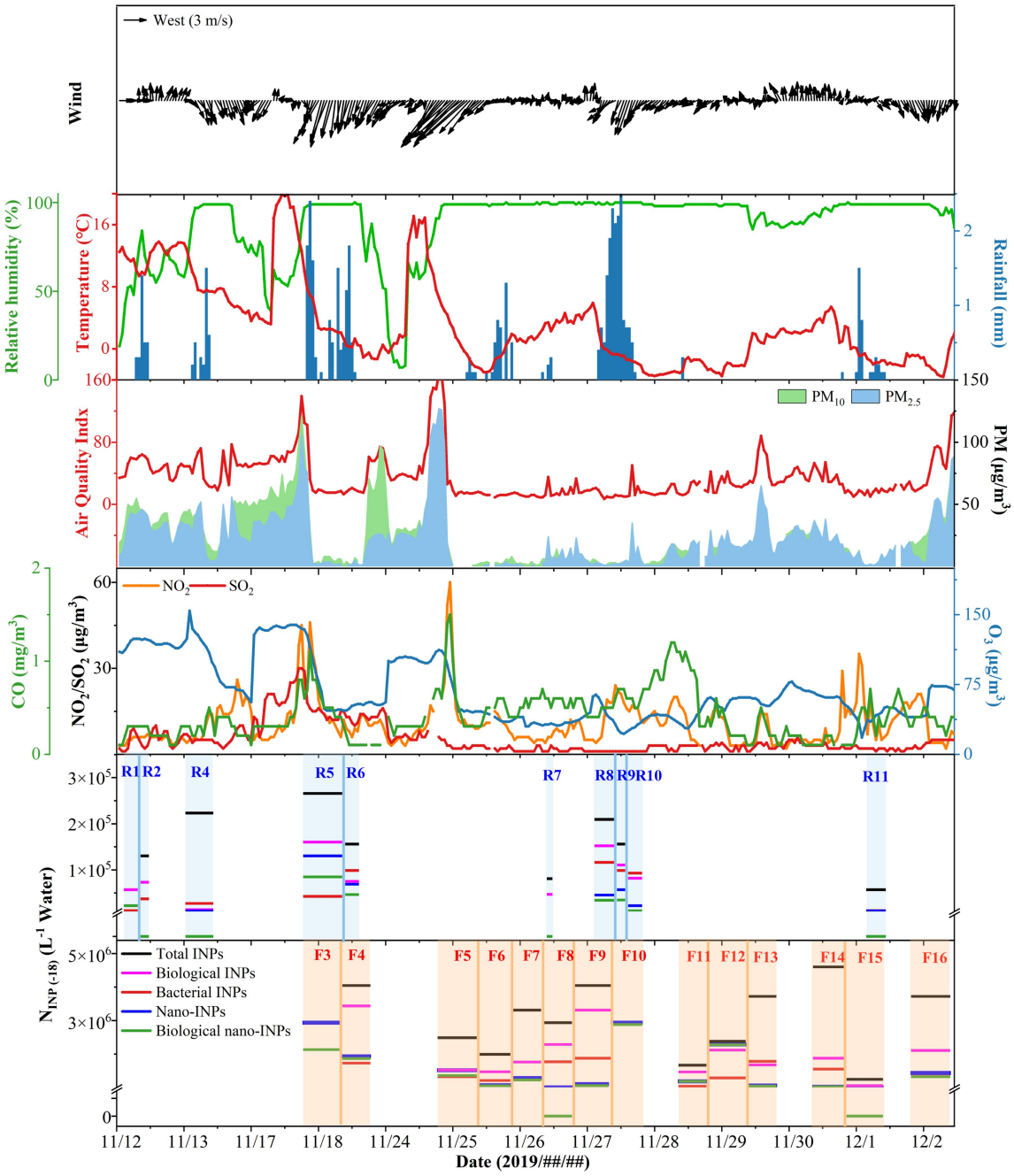

Figure S1. Data of environmental parameters (wind speed, wind direction, air temperature, relative humidity, rainfall, particulate matter (PM), NO_2, SO_2, O_3 and CO) during the sampling period and the concentrations of different types of INPs. For the sample IDs, F and R denote fog water and rainwater samples, respectively. F1, F2, and R3 were omitted from analyses due to small precipitation amounts.

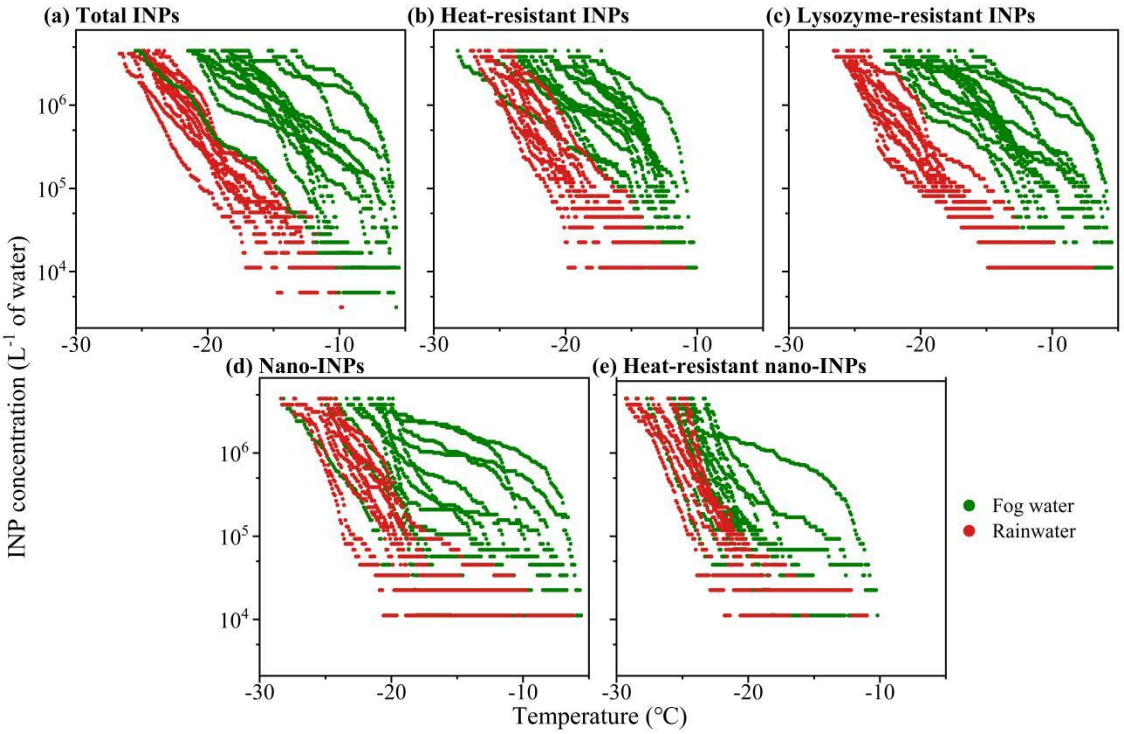

Figure S2. Comparisons of the total ice nucleating particles (INPs) spectra with heat-resistant INP spectra, lysozyme-resistant INPs spectra, nano-INPs spectra, and heat-resistant nano-INPs spectra obtained from rainwater samples (red dots) and fog water samples (green dots).

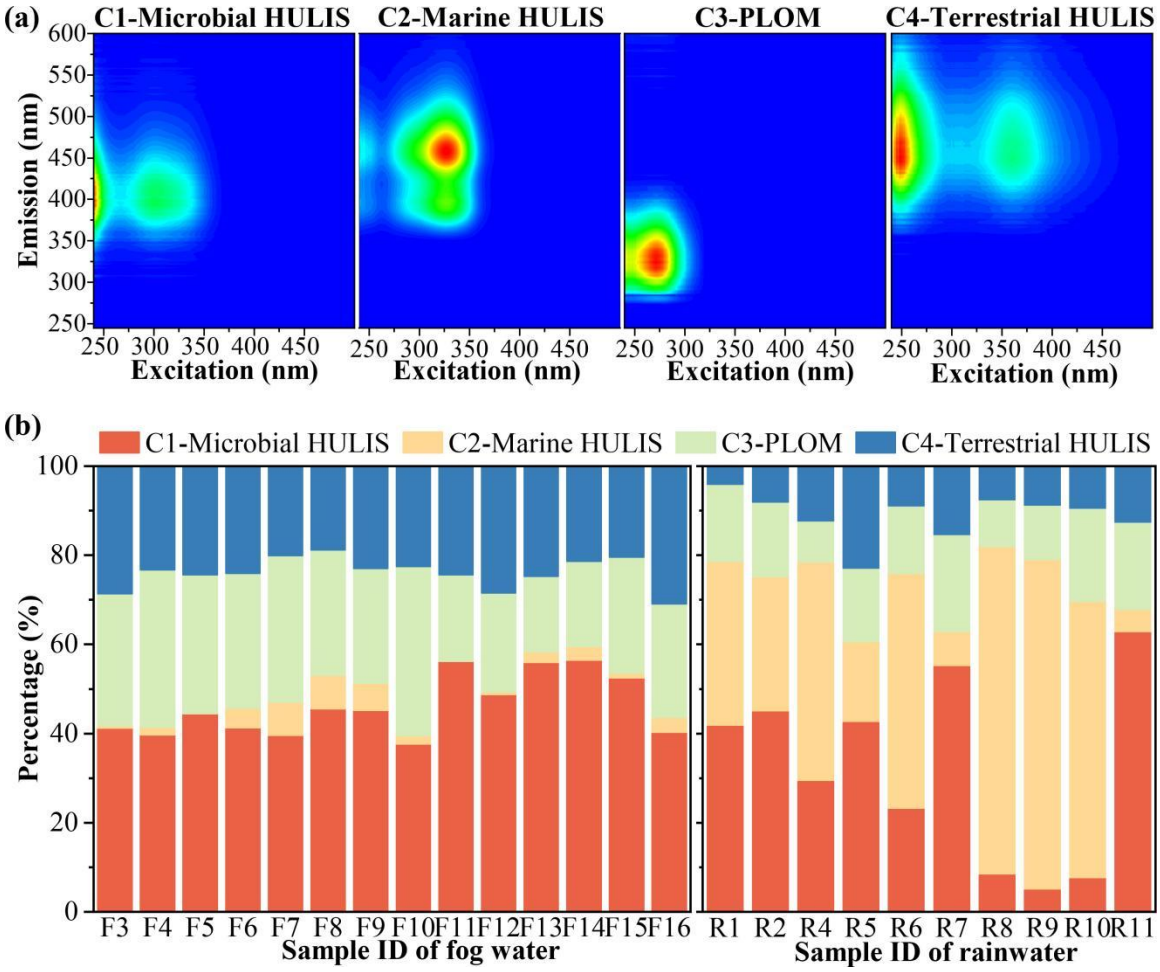

Figure S3. Fluorescence signatures of four components (C1-C4) and their percentages in the precipitation samples resolved by EEM fluorescent spectroscopy combined with PARAFAC analysis.

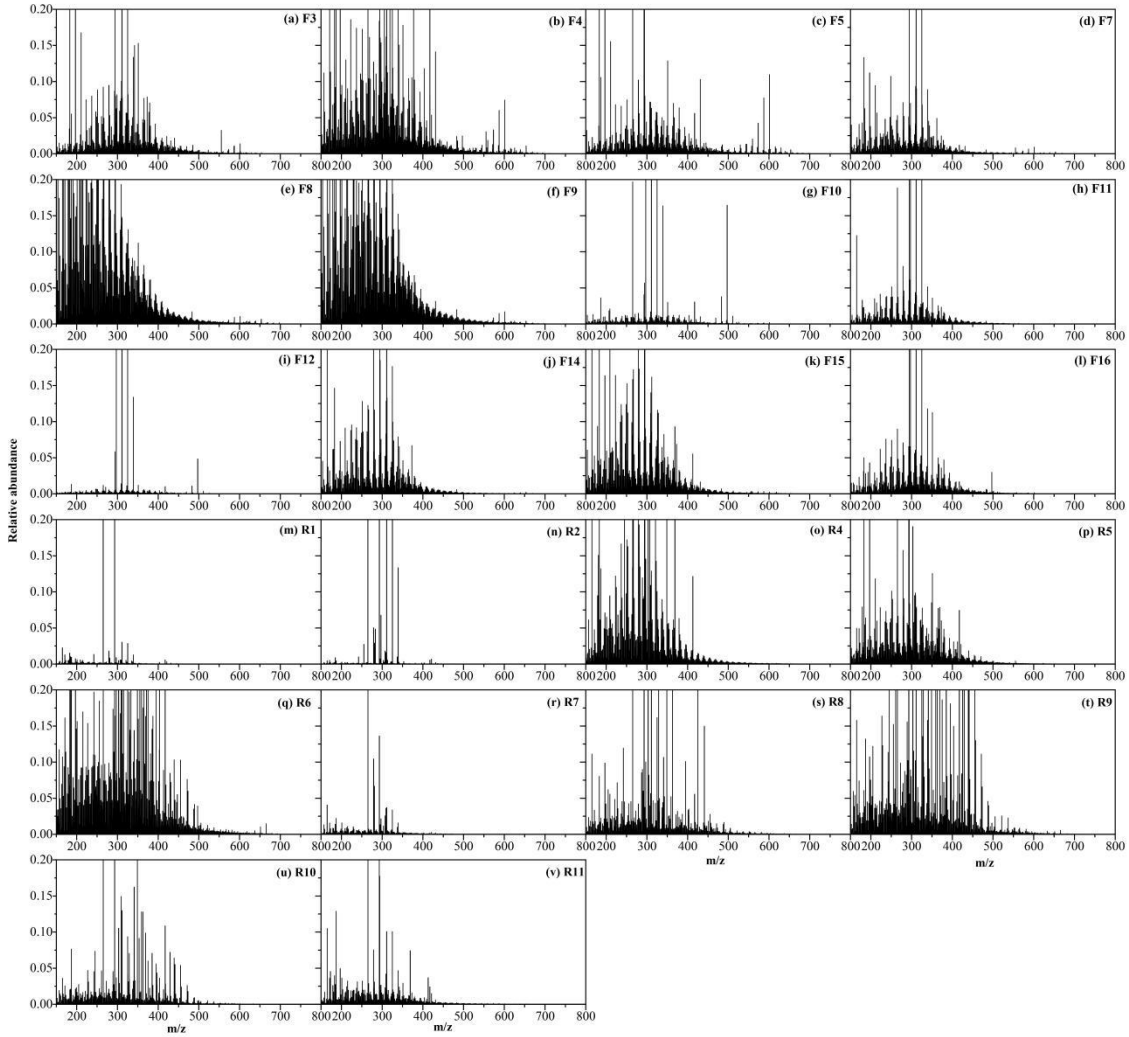

Figure S4. Reconstructed Fourier-transform ion cyclotron resonance mass spectra for 12 fog samples and 10 rainwater samples.

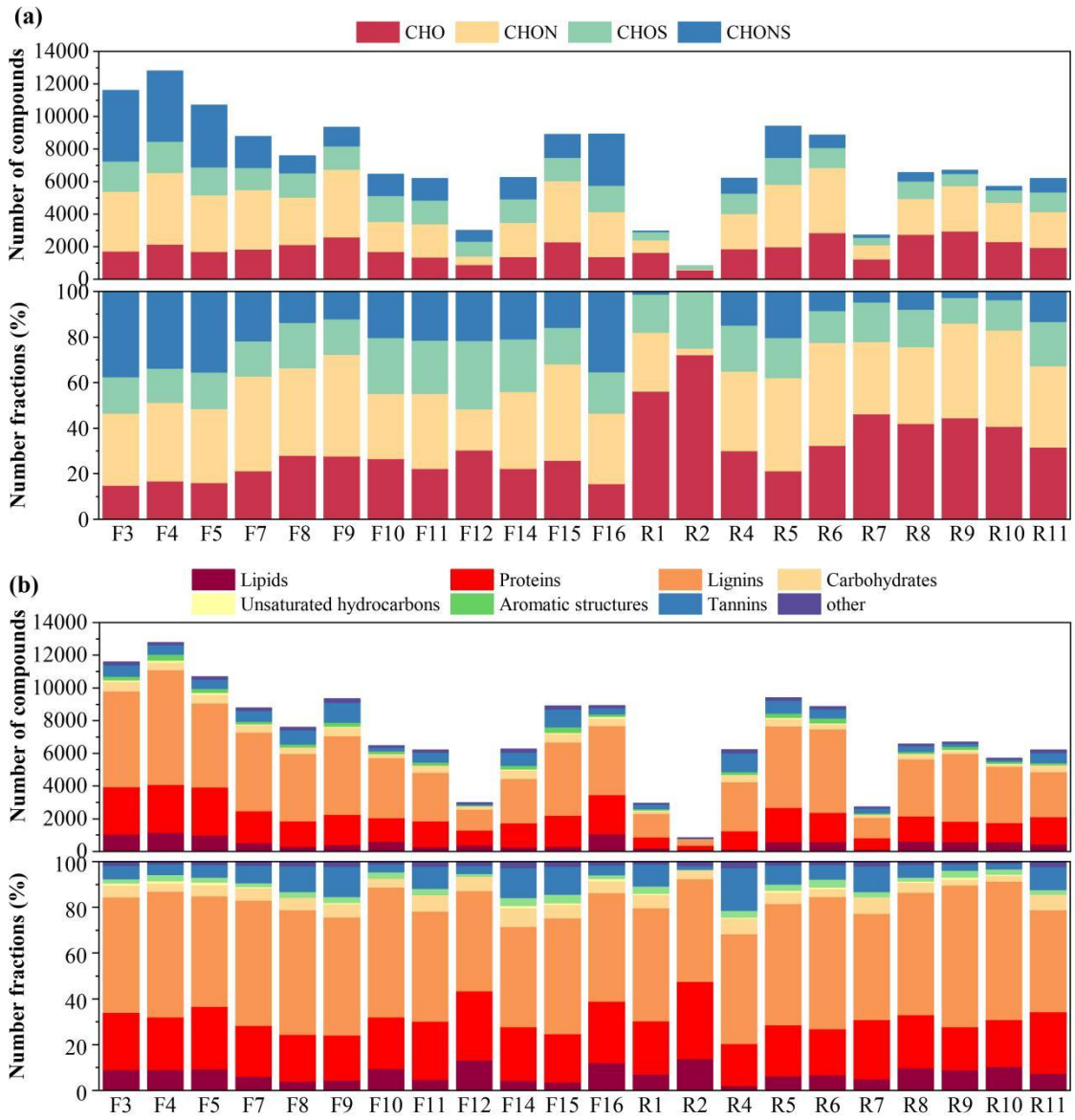

Figure S5. The total numbers and number fractions of (a) CHO, CHON, CHOS and CHONS, and (b) lipids, proteins, lignins, carbohydrates, unsaturated hydrocarbons, aromatic structures and tannins compounds in the precipitation samples.

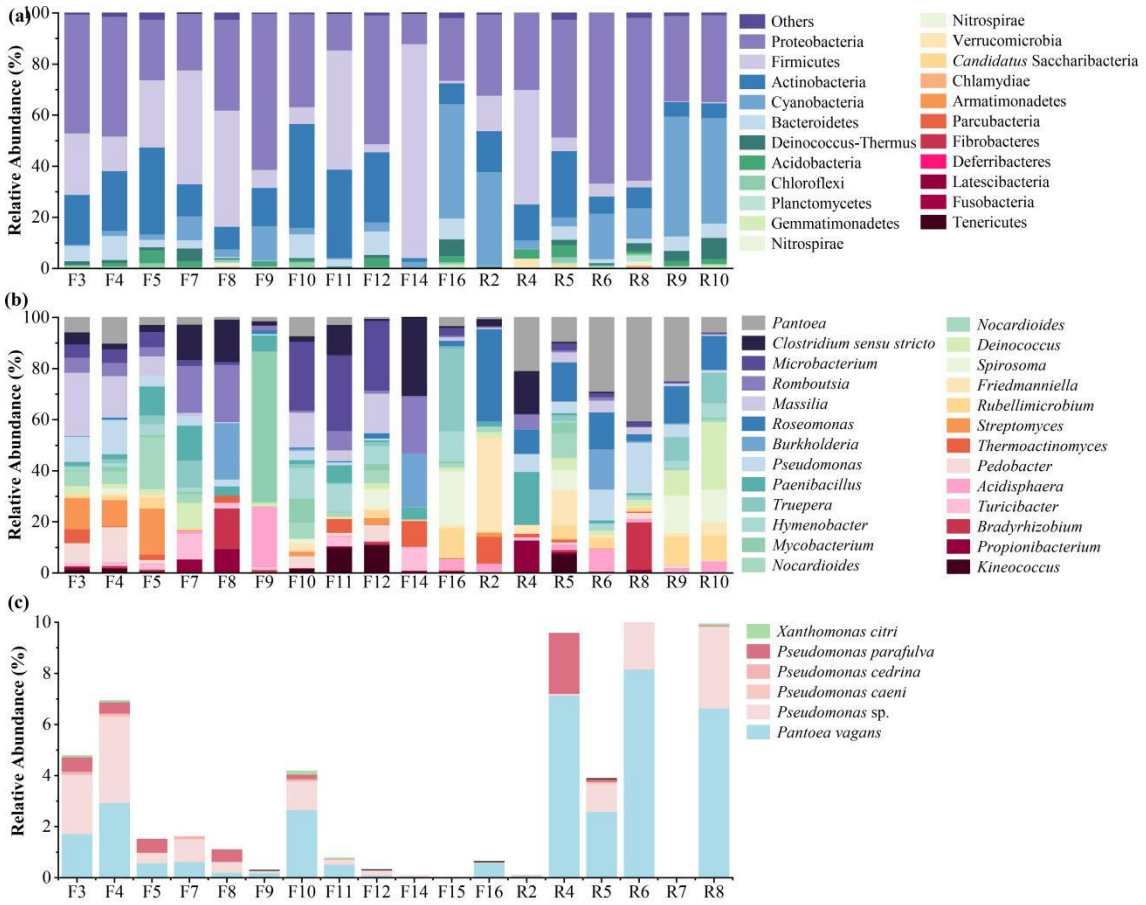

Figure S6. Relative abundances of the bacterial dominant (a) phyla, (b) genera and (c) the known INA species.

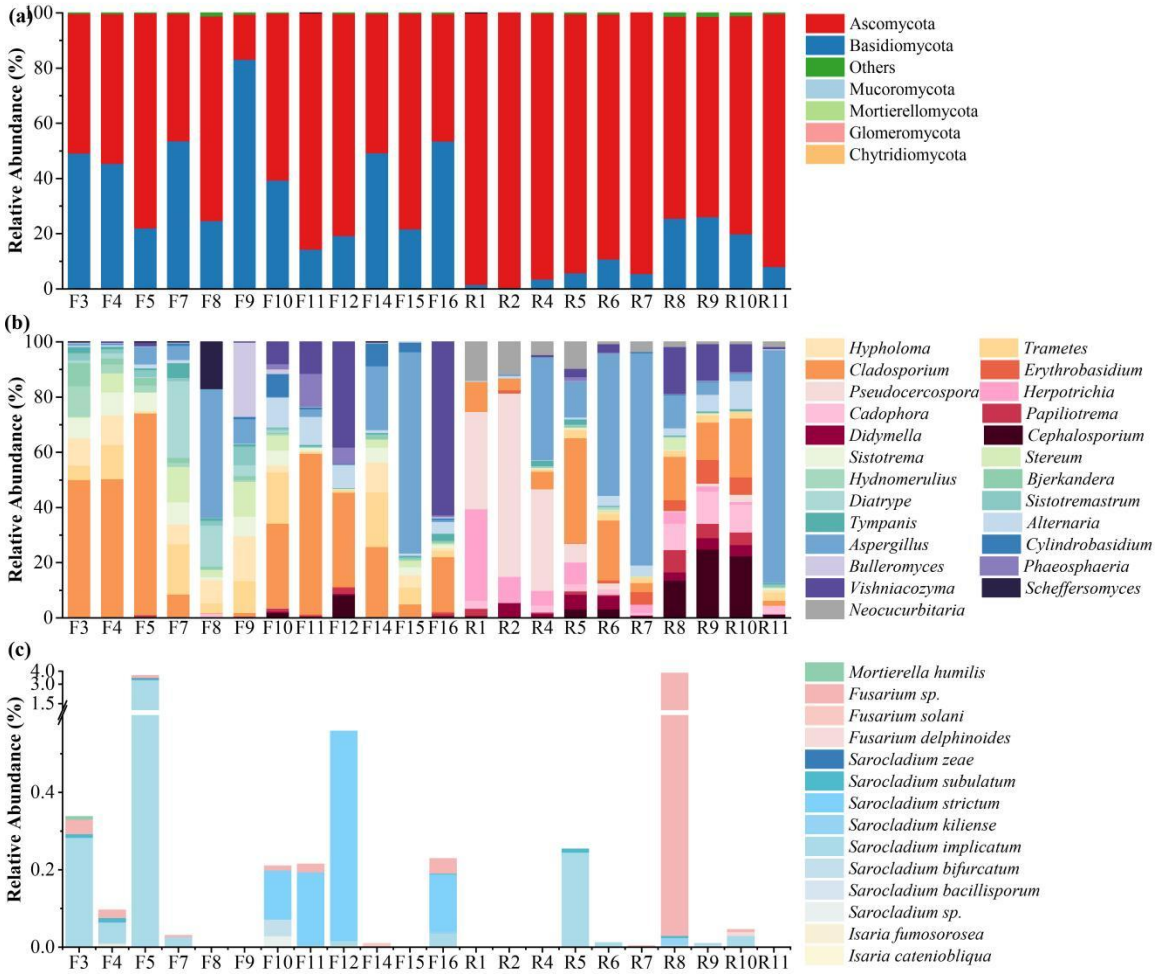

Figure S7. Relative abundances of the fungal dominant (a) phyla, (b) genera and (c) the known INA species.

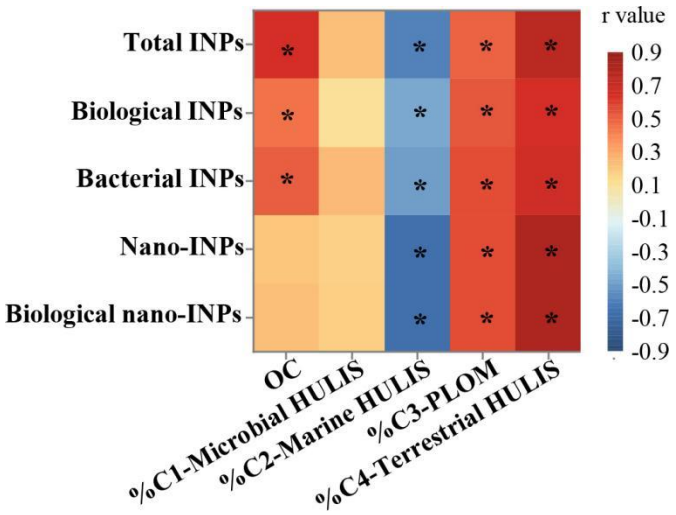

Figure S8. Spearman correlation heatmap of different types of INPs with (a) cations, (b) anions and (c) fluorescent components observed based on EEM data. The marker * represents the correlation that has significance at a *p*-value < 0.05.

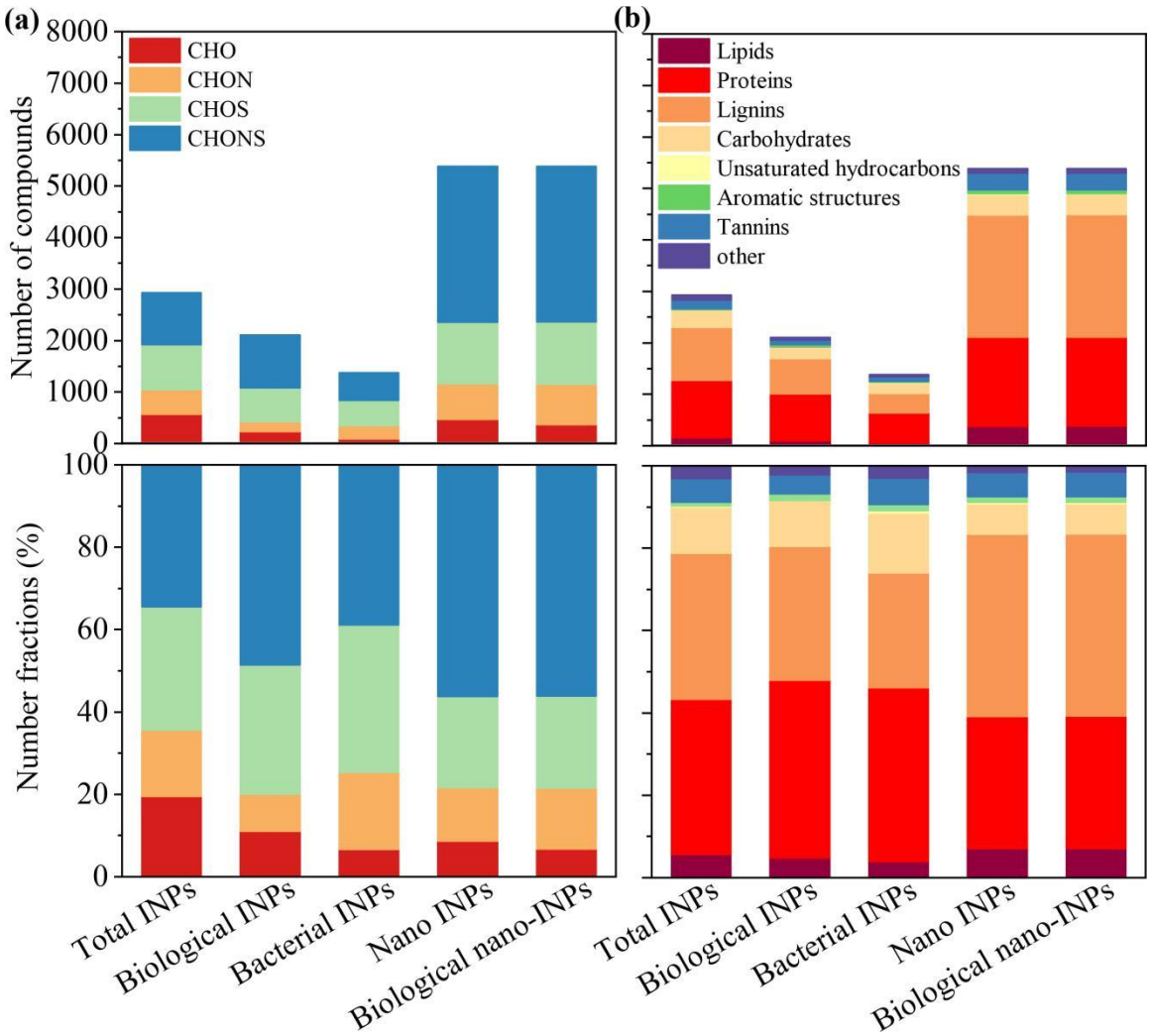

Figure S9. The total numbers and number fractions of (a) CHO, CHON, CHOS and CHONS, and (b) lipids, proteins, lignins, carbohydrates, unsaturated hydrocarbons, aromatic structures and tannins compounds related with different types of INPs based on Spearman's correlation analysis.

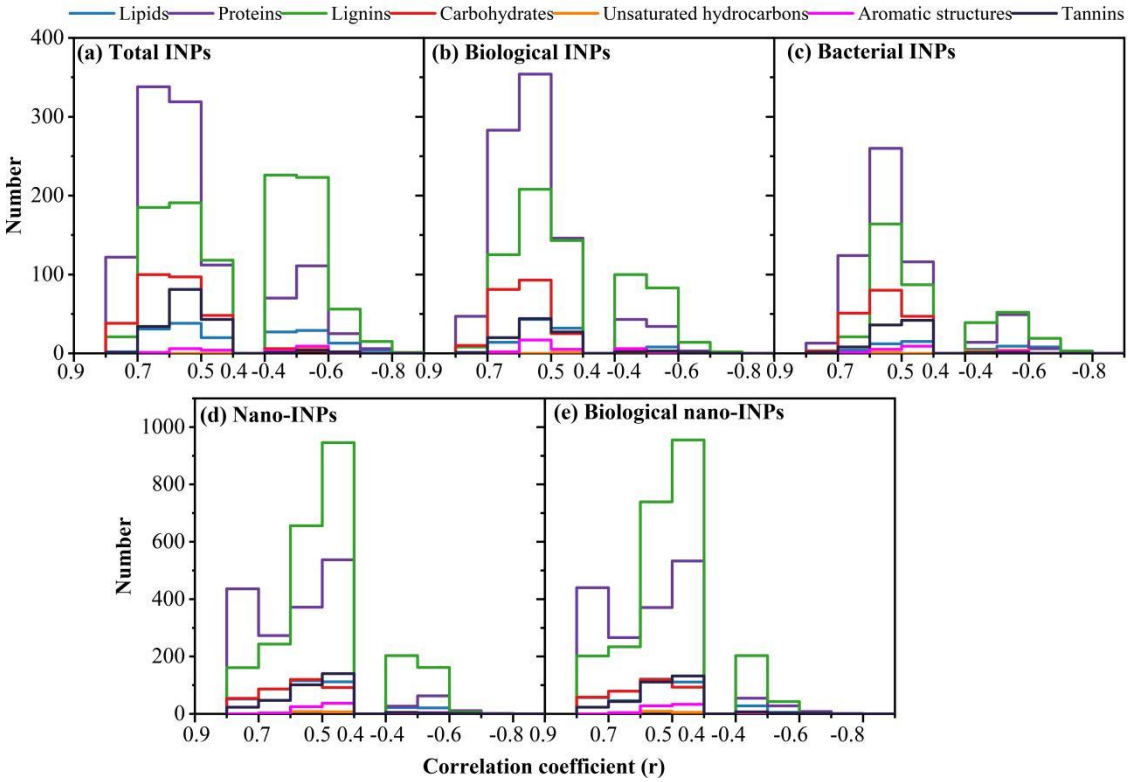

Figure S10. Correlation coefficient distribution of lipids, proteinaceous matter, lignins, carbohydrates, unsaturated hydrocarbons and tannins compounds with different types of INPs.

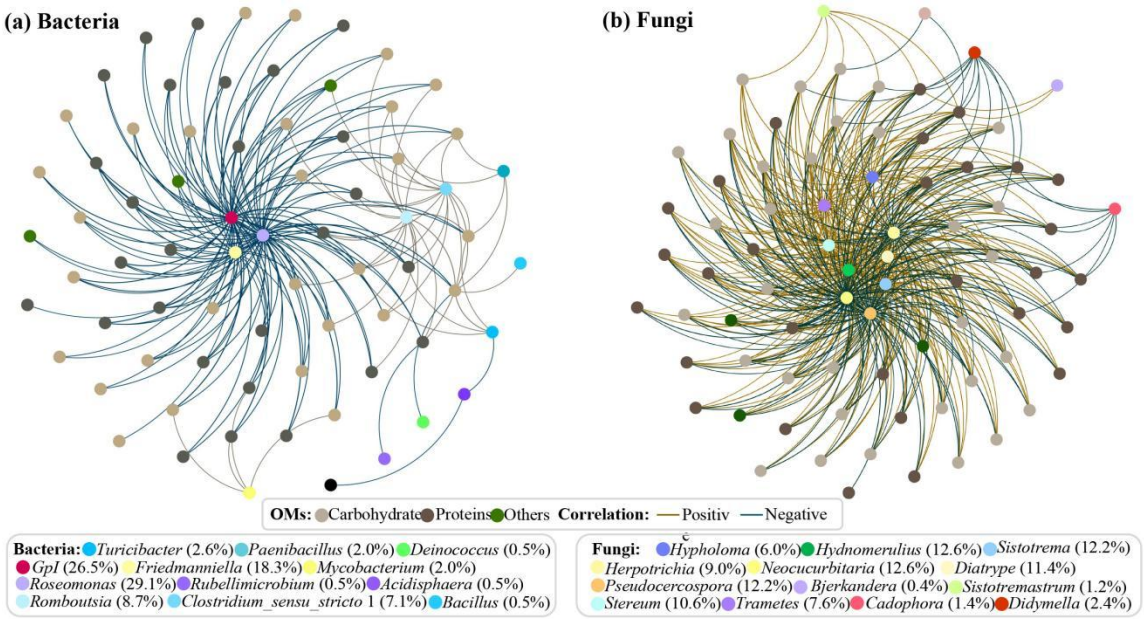

Figure S11. Co-occurrence analysis of the (a) bacterial and (b) fungal genera with OM molecules related to biological INPs (correlation coefficient > 0.7) based on Spearman's correlation analysis.

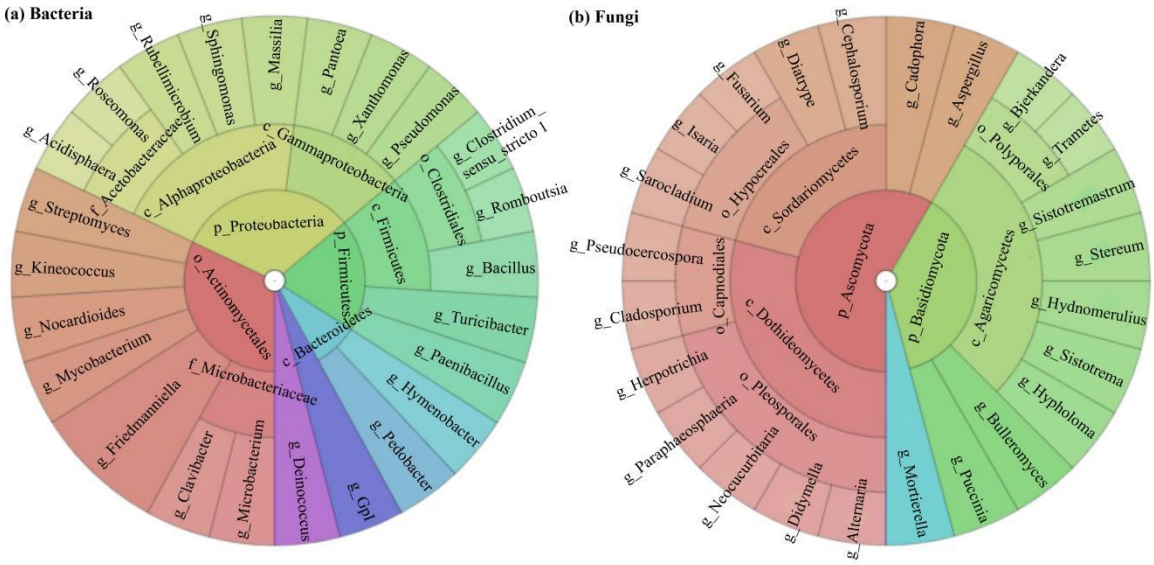

Figure S12. Krona diagram showing the taxonomic composition of the (a) bacterial and (b) fungal genera included in the co-occurrence network constructed between OM molecules associated with INPs (r values > 0.7) and microorganisms.

Table S1. The onset freezing temperature (T_0) and the temperature at which 50% of the droplets (T_{50}) of different types of INPs.

Sample	Sampling date (2019/##/## UTC+8:00)		INPs		Heat-resistant INPs		Lysozyme-resistant INPs		Nano-INPs		Heat-resistant nano-INPs	
ID	Start time	Stop time	T_0	T_{50}	T_0	T_{50}	T_0	T_{50}	T_0	T_{50}	T_0	T_{50}
F3	11/17 18:00	11/18 8:00	-5.8	-10.6	-10.2	-12.1	-5.5	-11.5	-6.2	-11.5	-10.6	-15.5
F4	11/18 8:30	11/18 16:30	-5.6	-7.7	-10.1	-16.8	-5.6	-8.7	-5.7	-11.8	-10.2	-23.9
F5	11/24 19:00	11/25 8:30	-7.6	-13.4	-11.2	-15.5	-7.6	-14.7	-10.3	-18.2	-11.7	-22.2
F6	11/25 8:30	11/25 20:00	-7.1	-14.4	-11.2	-18.2	-7.1	-14.9	-8.3	-19.7	-15.7	-23.1
F7	11/25 20:00	11/26 8:00	-7.0	-13.8	-11.8	-14.2	-7.9	-14.1	-8.1	-19.3	-12.7	-23.9
F8	11/26 8:30	11/26 19:30	-8.2	-15.1	-11.9	-17.2	-8.8	-15.6	-15.5	-21.7	-18.0	-24.4
F9	11/26 19:30	11/27 8:30	-6.0	-12.4	-11.9	-16.2	-6.2	-14.2	-7.5	-20.6	-12.8	-22.7
F10	11/27 8:30	11/27 19:30	-5.5	-7.5	-10.1	-14.6	-5.5	-8.0	-5.6	-8.7	-15.2	-21.5
F11	11/28 8:30	11/28 19:30	-6.0	-16.4	-12.7	-19.7	-6.0	-16.8	-8.7	-20.2	-19.2	-23.1
F12	11/28 20:00	11/29 8:30	-6.2	-12.1	-10.7	-19.3	-6.4	-13.9	-6.5	-12.8	-16.3	-22.0
F13	11/29 8:30	11/29 19:00	-5.9	-14.5	-10.4	-15.0	-6.4	-14.9	-8.6	-19.5	-16.6	-22.7
F14	11/30 8:30	11/30 19:30	-10.2	-14.0	-10.9	-14.8	-10.2	-14.7	-10.2	-19.6	-18.3	-23.9
F15	11/30 19:30	12/01 9:30	-11.2	-20.1	-13.5	-22.1	-11.4	-19.2	-16.1	-24.4	-18.0	-25.8
F16	12/01 19:30	12/02 9:00	-6.0	-13.0	-10.3	-15.4	-6.0	-14.3	-6.5	-18.2	-16.4	-20.1
Fog			**-7.0**	**-13.2**	**-11.2**	**-16.5**	**-7.2**	**-14.0**	**-8.8**	**-17.6**	**-15.1**	**-22.5**
R1	11/12 2:00	11/12 7:30	-14.1	-23.9	-19.3	-24.3	-12.8	-23.6	-11.0	-25.1	-21.4	-26.4
R2	11/12 7:30	11/12 11:00	-14.8	-22.8	-15.6	-23.0	-14.3	-23.0	-18.2	-24.8	-18.2	-25.1
R4	11/13 0:00	11/13 9:00	-9.8	-20.6	-11.5	-20.2	-11.8	-21.2	-15.5	-23.9	-17.2	-24.4
R5	11/17 18:00	11/18 7:00	-10.0	-20.0	-12.0	-21.2	-11.0	-20.6	-10.1	-21.3	-11.0	-23.6
R6	11/18 9:00	11/18 13:00	-9.6	-20.0	-12.5	-23.2	-10.9	-20.8	-12.9	-21.5	-16.9	-24.1
R7	11/26 9:00	11/26 10:00	-11.7	-19.8	-14.0	-24.1	-13.2	-20.1	-14.2	-20.4	-18.2	-25.7
R8	11/27 2:00	11/27 8:00	-10.4	-20.4	-11.4	-21.9	-14.0	-21.9	-12.3	-22.1	-14.7	-23.9
R9	11/27 10:00	11/27 12:00	-11.8	-21.9	-13.0	-23.5	-12.7	-23.3	-6.2	-23.2	-15.5	-23.5
R10	11/27 14:00	11/27 18:00	-10.0	-21.6	-12.4	-22.7	-10.8	-22.7	-11.3	-22.5	-16.9	-23.5
R11	12/01 4:00	12/01 9:30	-12.4	-21.2	-14.4	-21.4	-13.5	-22.8	-17.3	-22.7	-17.9	-24.5
Rain			**-11.5**	**-21.2**	**-13.6**	**-22.6**	**-12.5**	**-22.0**	**-12.9**	**-22.8**	**-16.8**	**-24.5**

Table S2. Spearman correlation between different types of INPs and the number of different categories of organic molecular formulas assigned according to the elemental compositions.

Types of INPs	CHO	CHON	CHOS	CHONS	Total formulas
Total INPs	-0.04	0.43	0.78**	0.77**	0.63**
Biological INPs	-0.01	0.41	0.69**	0.62**	0.52*
Bacterial INPs	0.17	0.29	0.58**	0.46*	0.52*
Nano-INPs	-0.33	0.19	0.59**	0.64**	0.37
Biological nano-INPs	-0.37	0.14	0.59**	0.64**	0.33

Note: * $p < 0.05$, ** $p < 0.01$

Table S3. The information of OM molecules exhibiting negative correlations with INPs. The possible naming of compounds was provided.

m/z	OM formula	H/C	O/C	R^2	Possible molecule
186	$C_9H_{17}NO_3$	1.89	0.33	-0.56	Ac-Ile-OMe
230	$C_{11}H_{21}NO_4$	1.91	0.36	-0.51	Boc-D-Ile-OH
244	$C_{12}H_{23}NO_4$	1.92	0.33	-0.54	Boc-D-Leu-OMe
202	$C_9H_{17}NO_4$	1.89	0.44	-0.56	Ac-Ser(tBu)-OH Boc-N-methyl-L-alanine
284	$C_{12}H_{19}N_3O_5$	1.58	0.42	-0.62	H-Gly-Pro-Hyp-OH
257	$C_{12}H_{22}N_2O_4$	1.83	0.33	-0.63	Boc-Pro-NMe(OMe)
286	$C1_2H_{21}N_3O_5$	1.75	0.42	-0.61	Ac-Ala-Ala-Ala-OMe
170	$C_9H_{17}NO_2$	1.89	0.22	-0.55	H-D-Pro-OtBu
442	$C_{21}H_{37}N_3O_7$	1.76	0.33	-0.47	Boc-Lys(Boc)-Pro-OH
245	$C_{10}H_{18}N_2O_5$	1.80	0.50	-0.59	Boc-Gln-OH
287	$C_{13}H_{24}N_2O_5$	1.85	0.38	-0.48	Boc-Leu-Gly-OH
411	$C_{23}H_{28}N_2O_5$	1.22	0.22	-0.47	Z-Phe-Leu
425	$C_{23}H_{26}N_2O_6$	1.13	0.26	-0.61	Boc-D-Gln(Xan)-OH